

# Global trench migration velocities and slab migration induced upper mantle volume fluxes: Constraints to find an Earth reference frame based on minimizing viscous dissipation

W.P. Schellart<sup>a,\*</sup>, D.R. Stegman<sup>b</sup>, J. Freeman<sup>a,1</sup>

<sup>a</sup> *Research School of Earth Sciences, The Australian National University, Canberra, ACT 0200, Australia*

<sup>b</sup> *School of Mathematical Sciences, Monash University, Melbourne, VIC 3800, Australia*

Received 22 August 2007; accepted 18 January 2008

Available online 13 February 2008

## Abstract

Since the advent of plate tectonics different global reference frames have been used to describe the motion of plates and trenches. The difference in plate motion and trench migration between different reference frames can be substantial (up to 4 cm/yr). This study presents an overview of trench migration velocities for all the mature and incipient subduction zones on Earth as calculated in eight different global reference frames. Calculations show that, irrespective of the reference frame: (1) trench retreat always dominates over trench advance, with 62–78% of the 244 trench segments retreating; (2) the mean and median trench velocity are always positive (retreating) and within the range 1.3–1.5 cm/yr and 0.9–1.3 cm/yr, respectively; (3) rapid trench retreat is only observed close to lateral slab edges (<1500 km); and (4) trench retreat is always slow far from slab edges (>2000 km). These calculations are predicted by geodynamic models with a varying slab width, in which plate motion, trench motion and mantle flow result from subduction of dense slabs, suggesting that trench motion is indeed primarily driven by slab buoyancy forces and that proximity to a lateral slab edge exerts a dominant control on the trench migration velocity. Despite these four general conclusions, significant differences in velocities between such reference frames remain. It is therefore important to determine which reference frame most likely describes the true absolute velocities to get an understanding of the forces driving plate tectonics and mantle convection. It is here proposed that, based on fluid dynamic considerations and predictions from geodynamic modelling, the best candidate is the one, which optimises the number of trench segments that retreat, minimizes the trench–perpendicular trench migration velocity ( $v_{T\perp}$ ) in the centre of wide (>4000 km) subduction zones, maximizes the number of retreating trench segments located within 2000 km of the closest lateral slab edge, minimizes the average of the absolute of the trench–perpendicular trench migration velocity ( $|v_{T\perp}|$ ) for all subduction zones on Earth, and minimizes the global upper mantle toroidal volume flux ( $\phi_{To}$ ) that results from trench migration and associated lateral slab migration (i.e. slab rollback or slab roll-forward). Calculations show that these conditions are best met in one particular Indo-Atlantic hotspot reference frame, where 75% of the subduction zones retreat,  $v_{T\perp}$  in the centre of wide subduction zones ranges between –3.5 and 1.8 cm/yr, 83% of the trench segments located within 2000 km of the closest lateral slab edge retreat, the average of  $|v_{T\perp}|$  is 2.1 cm/yr, and  $\phi_{To} = 456 \text{ km}^3/\text{yr}$  (lower limit) and  $539 \text{ km}^3/\text{yr}$  (upper limit). Inclusion of all the incipient subduction zones on Earth results in slightly greater fluxes of  $465 \text{ km}^3/\text{yr}$  (lower limit) and  $569 \text{ km}^3/\text{yr}$  (upper limit). It is also found that this reference frame is close to minimizing the total sub-lithospheric upper mantle volume flux ( $\phi_K$ ) associated with motion of continental keels located below the major cratons. It is stressed, however, that  $\phi_K$  is an order of magnitude smaller than  $\phi_{To}$ , and thus of subordinate importance. In conclusion, the Indo-Atlantic hotspot reference frame appears preferable for calculating plate velocities and plate boundary velocities.

© 2008 Elsevier B.V. All rights reserved.

**Keywords:** plate tectonics; subduction; reference frame; viscous dissipation; mantle convection; hotspot

\* Corresponding author. School of Geosciences, Monash University, Melbourne VIC 3800, Australia. Tel.: +61 3 9905 1782; fax: +61 3 9905 4903.

E-mail address: [wouter.schellart@sci.monash.edu.au](mailto:wouter.schellart@sci.monash.edu.au) (W.P. Schellart).

<sup>1</sup> Now at: Bureau of Meteorology, GPO Box 1289, Melbourne, VIC 3001, Australia.

## 1. Introduction

### 1.1. Different global reference frames

Knowledge of the absolute motion of plates and plate boundaries on Earth is important in understanding the driving forces of plate tectonics and mantle convection. Different global reference frames have been used in the past to describe the “absolute” motion of plates and plate boundaries (e.g. [Minster and Jordan, 1978](#); [Chase, 1978](#); [Jarrard, 1986](#); [Garfunkel et al., 1986](#); [Gordon and Jurdy, 1986](#); [Müller et al., 1993](#); [Gripp and Gordon, 2002](#); [Heuret and Lallemand, 2005](#); [Sdrolias and Müller, 2006](#)). The most prominent ones include hotspot reference frames, no-net-rotation reference frames, reference frames that are attached to a specific tectonic plate, and paleomagnetic reference frames.

Hotspot reference frames are based on the hypothesis that hotspot trails observed at the Earth’s surface are caused by hot plumes that originate in the lower mantle or at the core–mantle boundary. Initially, it was thought that all the hotspots on Earth are fixed relative to one another ([Morgan, 1971](#)). It has since been shown that significant motion between the group of hotspots in the Indo-Atlantic region and the group of hotspots in the Pacific region has occurred in the Late Cretaceous and Cenozoic ([Molnar and Stock, 1987](#); [DiVenere and Kent, 1999](#); [Raymond et al., 2000](#)). Some authors question such relative motion and ascribe the apparent motion to non-quantified deformation along an ill-defined plate boundary in the Antarctic or Pacific region ([Duncan, 1981](#); [Acton and Gordon, 1994](#)). In any case, two different hotspot reference frames are now common, one that is based on the Pacific hotspots ([Gripp and Gordon, 1990, 2002](#); [Wessel et al., 2006](#)) and one that is based on the Indo-Atlantic hotspots ([Müller et al., 1993](#); [O’Neill et al., 2005](#)). It has also been proposed that relative motion is not limited to motion between the two groups of hotspots, but occurs for hotspots within one group as well, with fast relative velocities in the Pacific ([Koppers et al., 2001](#)) and much slower relative velocities in the Indo-Atlantic region ([O’Neill et al., 2005](#)). Recent work has called into question such suggestions for inter-hotspot motion in the Pacific region ([Wessel et al., 2006](#)).

The no-net-rotation reference frame is based on the geodynamic concept of no-net-torque ([Solomon and Sleep, 1974](#); [Minster and Jordan, 1974](#); [Argus and Gordon, 1991](#)). In its most simple form it assumes uniform lithosphere–asthenosphere drag and symmetrical plate boundary torques. One well-known reference frame is the one from [Argus and Gordon \(1991\)](#), which uses the relative plate motion model of [DeMets et al. \(1990\)](#). This relative plate motion model is defined primarily from fitting magnetic anomalies and fracture zones across spreading ridges and is averaged over the last 3 Myr. More recently, a no-net-rotation reference frame has been developed that uses a global set of relative plate motions determined with geodetic methods ([Kreemer and Holt, 2001](#); [Kreemer et al., 2003](#)). This new model takes into account the motion of microplates, such as in East and Southeast Asia, and diffuse deformation along plate boundaries, which had been ignored in previous studies.

Reference frames have also been based on a specific tectonic plate, thought to have been relatively stable due to, for example,

balancing of the driving forces along the entire circumference of the plate. [Hamilton \(2003\)](#) proposed that the Antarctic plate currently represents an absolute reference frame as he noted that it is completely surrounded by spreading ridges, which would keep the plate in place because the sum of the ridge push force for the entire circumference of the plate would be zero.

A fourth reference frame, which will not be considered in the calculations presented here, is the paleomagnetic reference frame, which is based on the axial geocentric dipole hypothesis. In this hypothesis the paleomagnetic poles are assumed to represent the ancient spin axis, under the assumption that the Earth’s magnetic field is dipolar and that the dipolar axis is coincident with the spin axis. This is the only reference frame that is available for times prior to the Mesozoic. Unfortunately, the reference frame only provides latitudinal positions, whilst longitudinal positions remain quantitatively unconstrained.

### 1.2. Criteria to find the best global reference frame

Plate velocities and plate boundary velocities can vary significantly between different reference frames and can amount up to 4 cm/yr ([Fig. 1](#)). In particular, velocities in the Pacific hotspot reference frame from [Gripp and Gordon \(2002\)](#) ([Fig. 1b](#)) differ substantially from those in both the Indo-Atlantic hotspot reference frame from [O’Neill et al. \(2005\)](#) ([Fig. 1a](#)) and the no-net-rotation reference frames such as the one from [Kreemer et al. \(2003\)](#) ([Fig. 1c](#)). These differences are truly significant, considering that velocities of the fast plates range between 6 and 12 cm/yr in such reference frames. It is of primary importance to extract which, if any, of these reference frames is most likely to describe the absolute velocity of plates and plate boundaries, in particular to gain insight into mantle convection patterns and the relative importance of different driving and resistive forces in plate tectonics. In this paper it is proposed that, based on fluid dynamic considerations and predictions from geodynamic modelling, the reference frame that meets the following four conditions will most closely approximate a true absolute reference frame on Earth:

- (1) First, the reference frame needs to optimise the number of trench segments that retreat and thus minimize the number of trenches that advance for all subduction zones on Earth. This condition is based on two lines of evidence. The first line of evidence comes from geodynamic modelling. Two-dimensional (e.g. [Zhong and Gurnis, 1995](#); [Buiter et al., 2001](#); [Enns et al., 2005](#)) and three-dimensional (e.g. [Kincaid and Olson, 1987](#); [Schellart, 2004a,b](#); [Stegman et al., 2006](#); [Funicello et al., 2006](#); [Morra et al., 2006](#); [Schellart et al., 2007](#)) geodynamic simulations of free subduction with mobile plates and trenches show that trenches predominantly retreat. In both 2D models and 3D models, the trench motion is always regressive in the first stage of subduction, before interaction between slab tip and upper–lower mantle transition zone ([Kincaid and Olson, 1987](#); [Zhong and Gurnis, 1995](#); [Schellart, 2004a,b](#); [Enns et al., 2005](#); [Stegman et al., 2006](#); [Funicello et al., 2006](#); [Schellart](#)

et al., 2007; Schellart, 2008). During and after the first interaction between slab tip and the transition zone, trench motion is predominantly regressive for a variety of subduction settings. In 2D models, exceptions occur during subduction of a very stiff slab (Enns et al., 2005) or at times when a slab pile flushes through the transition zone (Zhong and Gurnis, 1995). In 3D models trench advance is only observed in very specific tectonic settings: in the centre of wide (>4000 km) subduction zones (Schellart et al., 2007), but then only episodically and at slow velocities (not exceeding 2 cm/yr); in case the slab/mantle viscosity ratio is unrealistically high ( $1-5 \times 10^3$ ) (Schellart, 2008); or when the subducting plate is rapidly forced to move towards the subduction zone (Schellart, 2005). Note that trench advance velocities observed in all dynamic models are comparatively small, generally not more than  $\sim 3$  cm/yr, while trench retreat velocities can reach 10 cm/yr or more. Also note that in general, 2D models show slower trench retreat velocities than 3D models, which is explained by the greater efficiency in return flow for 3D models, where flow is allowed around the lateral edges of the slab.

The second line of evidence comes from the geometry of slabs. Predominant trench advance would produce roll-over slab geometries, which are very rare on Earth. There is only one clear example of a roll-over slab geometry, the Tethyan slab below the Himalayas (Van der Voo et al., 1999), which is a collision/continental subduction zone, not a normal subduction zone. At normal subduction zones, relatively steep (e.g. Mariana, New Britain, New Hebrides, and Kermadec), gentle (e.g. Hellenic), kinked (e.g. South America) or backward draping (e.g. Tonga, Calabria, and Kuril) slab geometries are observed. Such geometries point to trench retreat or slow episodic trench migration, not to predominant trench advance.

- (2) Second, the reference frame needs to minimize the trench migration velocity in the centre of wide subduction zones (>4000 km) and maximize the number of retreating trench segments located within 2000 km of the closest lateral slab edge. Note that the width of a subduction zone is here defined as its trench-parallel extent. Recent three-dimensional geodynamic modelling of subduction zones with a variable width (300–7000 km) shows that wide slabs (>4000 km) migrate slowly in the centre, while regions close to lateral slab edges, be it edges of narrow or wide slabs, almost invariably retreat (Schellart et al., 2007). Slow trench migration in the centre of wide subduction zones is explained by the long return flow path for mantle material from one side of the slab to the other side due to the large distance to the closest lateral slab edge. Near slab edges, the return flow path is much shorter, and thus lateral slab migration near slab edges will experience less mantle resistance, thereby facilitating slab rollback and trench retreat.
- (3) Third, partly following Kaula (1975), the reference frame needs to minimize the cumulative amount of the absolute trench-perpendicular trench migration velocity ( $|v_{T\perp}|$ ) for

all subduction zones on Earth. Flow patterns shift about more slowly than material velocities in convective systems due to some sort of work minimization (Kaula, 1975). For the Earth's convective mantle, work minimization indicates minimizing viscous dissipation. Such work minimization would be found in an Earth reference frame that minimizes the cumulative amount of plate boundary migration. Kaula (1975) also noted that one would expect sinks (subduction zones) to be more likely to remain fixed than sources (spreading ridges) because the material is much stiffer at sinks due to the temperature dependent viscosity of the convective materials. In addition, sources are considered to be passive features, i.e. passive upwelling from shallow, upper mantle depths (Davies, 1999), and thus only the sinks are important in minimizing viscous dissipation in the mantle. Note that the migration of transform plate boundaries is not considered either, because these are plate features that do not extend significantly into the sub-lithospheric mantle. From this it follows that the global sum of  $|v_{T\perp}|$  should be minimized, and that the number of rapidly advancing trenches and rapidly retreating trenches should also be minimized.

- (4) Fourth, following on from criterion three, the reference frame needs to minimize the global upper mantle toroidal volume flux ( $\phi_{T_o}$ ) that results from trench migration and lateral slab migration. Work minimization on Earth would be achieved by minimizing viscous dissipation in the mantle. Viscous dissipation associated with the subduction flux (poloidal flux) depends only on relative plate motions. Indeed, the global heat loss due to subduction is not dependent on the plate motions in the adopted absolute reference frame, but only on relative plate motions. Viscous dissipation associated with lateral-slab-migration-induced toroidal flow in the mantle (e.g. Kincaid and Griffiths, 2003; Schellart, 2004a; Funicello et al., 2006; Stegman et al., 2006; Schellart et al., 2007), however, does depend on the adopted reference frame. Recent modelling indicates that lateral slab migration induces a flow that occurs exclusively around the lateral slab edges and that lateral-slab-migration-induced poloidal return flow around the slab tip does not occur for subduction zones on Earth (Schellart, 2008). The magnitude of the toroidal volume flux depends on  $|v_{T\perp}|$ , the width of the slab, the depth extend of the slab and how  $|v_{T\perp}|$  varies along the trench and with depth. This global flux needs to be minimized in order to minimize viscous dissipation in the convective system.

In theory the fourth criterion is a more robust assessment of Kaula's (1975) work minimization hypothesis than the third criterion, but there is a greater uncertainty in estimating the global  $\phi_{T_o}$  than the global  $|v_{T\perp}|$ , due to uncertainty in depth extent of the slab, and, more importantly, potential variation of  $|v_{T\perp}|$  with depth. This is why both  $|v_{T\perp}|$  and  $\phi_{T_o}$  are calculated.

This paper presents a large overview of research on trench migration velocities and lateral slab-migration-induced volume fluxes that was started in 2004 and continued in the following

years (Schellart, 2004c; Schellart et al., 2006; Schellart, 2007a; Schellart et al., 2007). The velocity calculations and volume flux calculations were done for all mature subduction zones (Table 1) and incipient subduction zones (Table 2) on Earth in

eight different global reference frames. Furthermore, the paper presents the general findings from these calculations, discusses the implications of these findings for subduction zone dynamics and mantle convection, and compares these calculations with

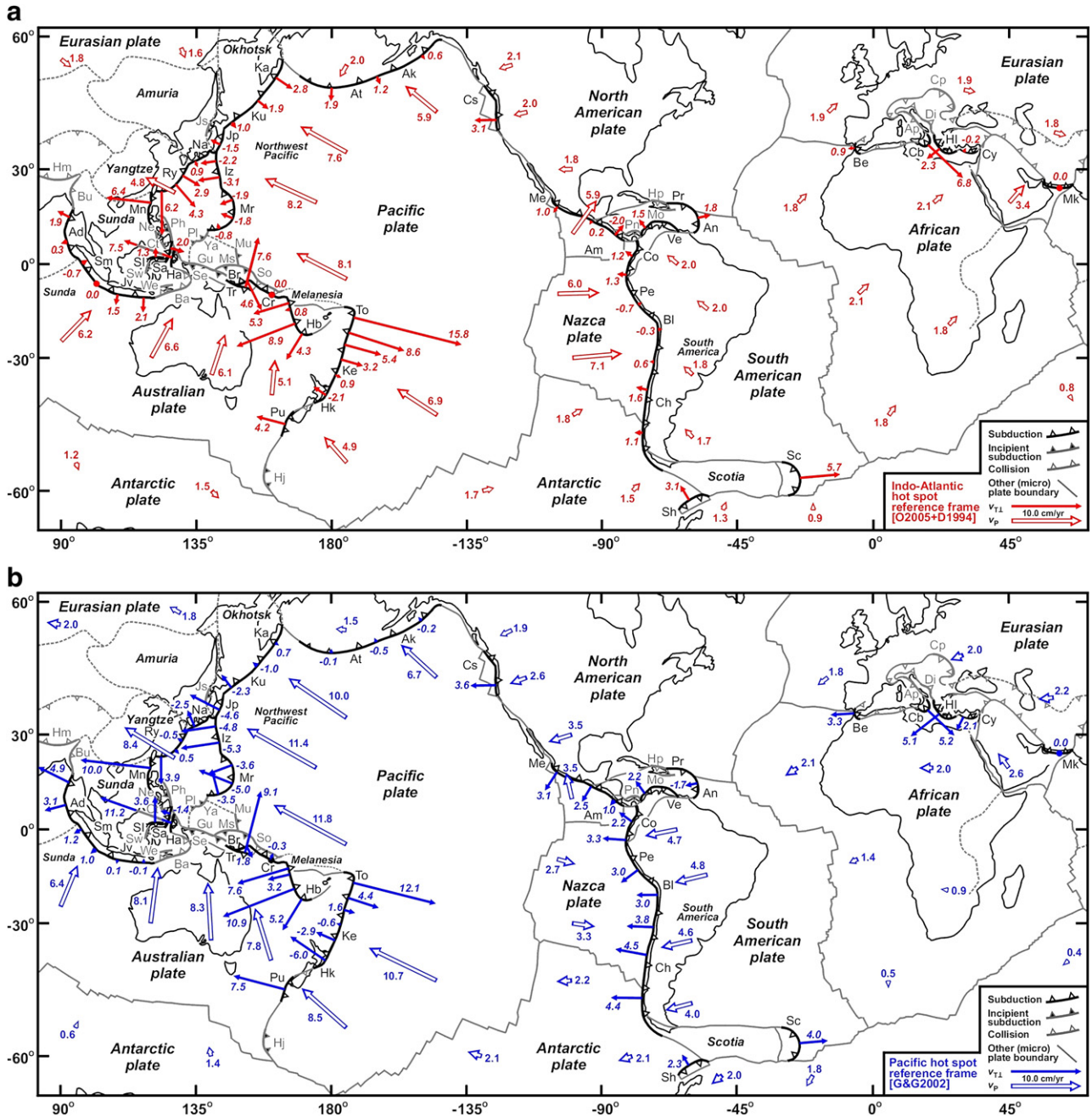


Fig. 1. Tectonic maps showing the major subduction zones on Earth, the velocities for the major plates ( $v_p$ ) and the trench–perpendicular trench migration velocities ( $v_{T\perp}$ ) in three global reference frames. (a) Indo-Atlantic hotspot reference frame of O’Neill et al. (2005) combined with the relative plate motion model of DeMets et al. (1994) (O2005+D1994) (modified from Schellart et al., 2007); (b) Pacific hotspot reference frame of Gripp and Gordon (2002) (G&G2002), who use the relative plate motion model of DeMets et al. (1994); (c) no-net-rotation reference frame of Kreemer et al. (2003) (K2003). Note that in Fig. 1a and b the arc/backarc deformation rates that are used are preferentially based on geology/geophysics, whilst in Fig. 1c rates are mostly based on geodetic investigations (see Methods section and Table 1 for more details). Also plotted are the incipient subduction zones. Subduction zones: Ad—Andaman, Ak—Alaska, Am—Central America, An—Lesser Antilles, At—Aleutian, Be—Betic-Rif, Bl—Bolivia, Br—New Britain, Cb—Calabria, Ch—Chile, Co—Colombia, Cr—San Cristobal, Cs—Cascadia, Cy—Cyprus, Ha—Halmahera, Hb—New Hebrides, Hk—Hikurangi, Hl—Hellenic, Iz—Izu-Bonin, Jp—Japan, Jv—Java, Ka—Kamchatka, Ke—Kermadec, Ku—Kuril, Me—Mexico, Mk—Makran, Mn—Manila, Mr—Mariana, Na—Nankai, Pe—Peru, Pr—Puerto Rico, Pu—Puysegur, Ry—Ryukyu, Sa—Sangihe, Sc—Scotia, Sh—South Shetland, Sl—North Sulawesi, Sm—Sumatra, To—Tonga, Tr—Trobriand, Ve—Venezuela. Collision zones: Ap—Apennines, Ba—Banda, Bu—Burma, Cp—Carpathian, Di—Dinarides, Hp—Hispaniola, Se—Seram, So—Solomon. Incipient subduction zones: Ct—Cotobato, Gu—New Guinea, Hj—Hjort, Js—Japan Sea, Mo—Mueertos, Ms—Manus, Mu—Mussau, Ne—Negros, Ph—Philippines, Pl—Palau, Pn—Panama, Sw—West Sulawesi, We—Wetar, Ya—Yap.

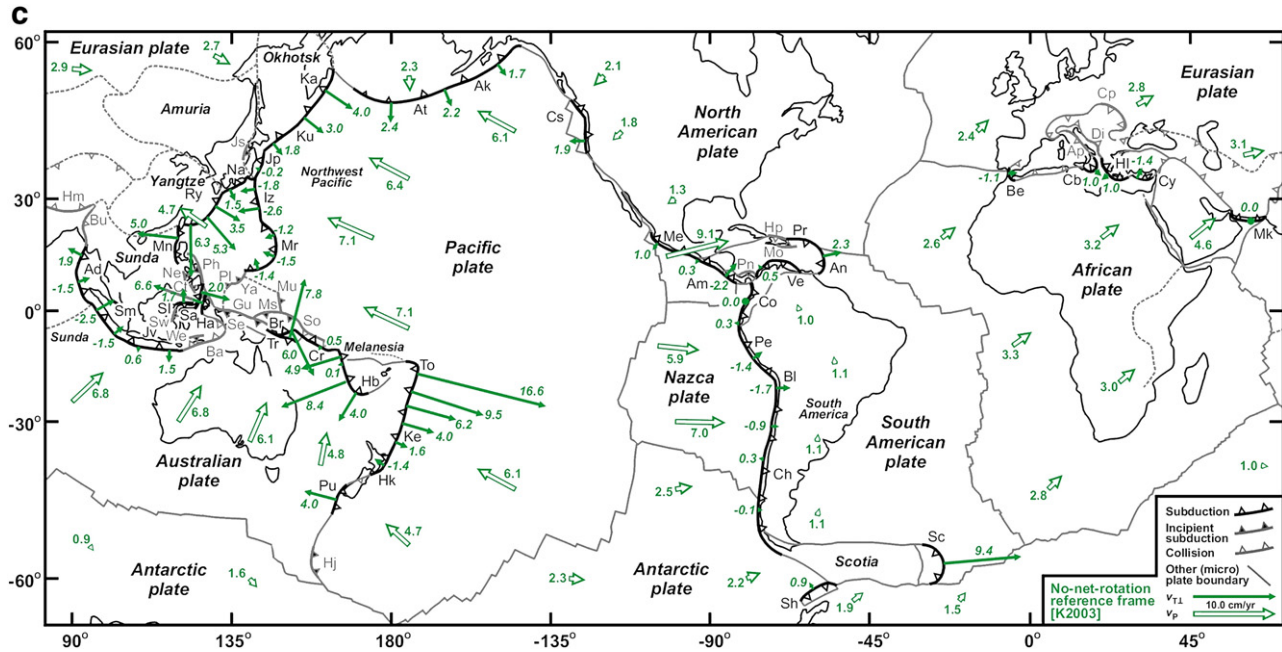


Fig. 1 (continued).

previous studies. Finally, the study shows which of these reference frames best meets the four criteria regarding trench migration and work minimization discussed above.

## 2. Methods

### 2.1. Calculations of trench migration velocity

The trench–perpendicular trench migration velocity ( $v_{T\perp}$ ) was calculated for a total of 24 mature subduction zones (Table 1) and 14 incipient subduction zones (Table 2). Each subduction zone was divided into individual trench segments with a length of 200 km, resulting in a total of 244 mature subduction zone trench segments and 52 incipient subduction zone trench segments. For each segment the trench–perpendicular component of the velocity was calculated. The size of the trench segments was chosen as such to have segments that are larger than the maximum thickness of subducting oceanic lithosphere, so more than  $\sim 100$  km, but not more than the width of the narrowest subduction zone. The trench–perpendicular trench migration velocity was calculated by summation of the following components: (1) the component of trench–perpendicular motion of the overriding plate in a global reference frame and potential microplate motion relative to the major plate ( $v_{OP\perp}$ ); (2) the component of trench–perpendicular overriding plate (permanent) deformation in the backarc/arc/fore-arc region ( $v_{OPD\perp}$ ); (3) the component of tectonic accretion/erosion of the overriding plate ( $v_{A\perp}$ ):

$$v_{T\perp} = v_{OP\perp} + v_{OPD\perp} + v_{A\perp}. \quad (1)$$

Note that by convention, trench retreat (rollback) is taken as positive, as are trenchward overriding plate motion and

microplate motion. Backarc/arc/fore-arc extension/spreading and accretion are also taken as positive. Motion for the major plates, microplates and most arc blocks was calculated from published rotation parameters (see Tables 1 and 2).

The overriding plate component of trench–perpendicular motion was calculated for the major overriding plates and potential microplates located in between the major plate and the subduction zone (see Table 3 for a list of plates and microplates used in this study). The motions of the major plates were calculated in three “fixed” hotspot reference frames (Gordon and Jurdy, 1986; Gripp and Gordon, 2002; Wessel et al., 2006), in the moving hotspot reference frame of O’Neill et al. (2005), in two no-net-rotation reference frames (Argus and Gordon, 1991; Kreemer et al., 2003) and in the Antarctic plate reference frame from Hamilton (2003). Gordon and Jurdy (1986), Argus and Gordon (1991), Gripp and Gordon (2002) and Kreemer et al. (2003) published the rotation parameters of all the major plates in their particular reference frame and these have been used here. The Antarctic plate reference frame from Hamilton (2003), the Pacific hotspot reference frame from Wessel et al. (2006) and the Indo-Atlantic hotspot reference frame from O’Neill et al. (2005) have been combined with the relative plate motion model from DeMets et al. (1994). In addition, the Indo-Atlantic hotspot reference frame from O’Neill et al. (2005) has also been combined with the relative plate motion model from Kreemer et al. (2003). This results in a total of eight different reference frames: G&J1986, A&G1991, G&G2002, K2003, H2003+D1994, O2005+D1994, O2005+K2003, W2006+D1994. Calculations that made use of the geodetic relative plate motion model from Kreemer et al. (2003) were combined mostly with geodetically derived  $v_{OPD\perp}$  estimates (24 out of a total of 28 overriding plate deformation rates), whilst the others were combined with geologically or geophysically derived  $v_{OPD\perp}$  estimates as much

Table 1  
Subduction zone data

Subduction system	Subduction zone width $\approx$ slab width (km)	Subduction zone edge or slab edge location	Maximum depth extent of seismic slab in upper mantle (km)	Maximum depth extent of tomographic slab in upper mantle (km)	Major overriding plate (+microplate) (+arc block) used to calculate trench velocity	Tectonic accretion (>0) or erosion (<0) (cm/yr)
Betic-Rif [Be]	250	N and S	600 (1)	670 (1)	EU-BE (1) <sup>a,b,c</sup>	?
Calabria [Cb]	300	NE and SW	500 (2)	670 (2)	EU-CB (3) <sup>a,b,d</sup>	?
South Shetland [Sh]	450	NE and SW	90 (4)	?	AN-SL (5) <sup>a,b,c</sup>	?
North Sulawesi [Sl]	500	E and W	300 (6)	?	EU-SU-MS (7, 8, 9) <sup>b</sup>	?
Halmahera [Ha]	500	N and S	250 (10)	670 (10)	AU-BH (7) <sup>b</sup>	?
Cyprus [Cy]	500	W and E	160 (11)	?	EU-AT (12) <sup>b</sup>	?
Puyssegur [Pu]	750	NE and SW	200 (13)	?	PA	?
Scotia [Sc]	800	N and S	350 (14)	670 (15)	AN-SC-SW (16) <sup>a,b,f</sup>	-0.5 (17)
Sangihe [Sa]	850	N and S	650 (10)	670 (10)	EU-SU (9) <sup>b</sup>	?
Trobriand [Tr]	900 <sup>g</sup>	E and W	150 (18)	200 (10)	AU-WL (19) <sup>b</sup>	?
Makran [Mk]	900	E and W	75 (20)	500 (15)	EU-MK (21) <sup>b</sup>	0.2 (22)
Manila [Mn]	1000	N and S	300 (23)	670 (24)	PS-(LU) (8) <sup>b</sup>	?
Cascadia [Cs]	1400	N and S	60 (25)	400 (25)	NA-(OR/NE) (26) <sup>a,b,h</sup>	0.2 (22)
Venezuela [Ve]	1550	E and W	160 (27)	300 (28)	SA-ND (7) <sup>a</sup>	?
Hellenic [Hl]	1700 <sup>i</sup>	SE and NW	200 (29)	670 (2)	EU-AT-AS (12) <sup>b</sup>	0.5 (22)
(Dinarides) [Di]						
Nankai [Na]	2250	SW	~100 (30)	~100 (30)	EU-AM-TK (9, 31) <sup>b</sup>	0.1 (22)
Ryukyu [Ry]			300 (32)	500 (24)	EU-YA-ON (33, 9) <sup>b</sup>	?
Lesser Antilles [An]	2450 <sup>j</sup>	N and S	220 (34)	670 (15, 35)	SA-CA (9) <sup>b</sup>	0.3 (22)
Puerto Rico [Pr]			210 (36)	?	SA-CA-HP (9, 36) <sup>b</sup>	?
(Hispaniola) [Hp]						
Mexico [Me]	3100	NW and SE	220 (37)	?	NA-ME (38) <sup>a</sup>	-0.1 (39)
Central America [Am]			250 (37)	?	NA-CA-(PM) (7, 9) <sup>b</sup>	-0.3 (40)
Aleutian [At]	3400	E and W	300 (37)	450 (41)	NA	0.1 (22)
Alaska [Ak]			250 (37)	?	NA	0.3 (22)
Tonga [To]	3550	N and S	670 (37)	670 (10, 42)	AU-TO (43) <sup>a,b</sup>	-0.4 (44)
Kermadec [Ke]			670 (37)	670 (10, 42)	AU-KE (7, 45) <sup>a,b</sup>	?
Hikurangi [Hk]			350 (46)	400 (46, 47)	AU-KE (7, 45) <sup>a,b</sup>	?
<i>Melanesia:</i>	4400 <sup>g</sup>	NW and SE				
New Britain [Br]			600 (18)	670 (10)	PA-SB (48) <sup>b</sup>	?
San Cristobal [Cr]			200 (49)	200 (10)	PA	?
N New Hebrides [Hb]			670 (10)	670 (10)	PA	?
C New Hebrides [Hb]			350 (37)	670 (10)	AU-NH (50) <sup>b,k</sup>	?
S New Hebrides [Hb]			300 (51)	500 (10)	AU-NH (50) <sup>b,k</sup>	?
<i>Northwest Pacific:</i>	6550	N and S				
Kamchatka [Ka]			650 (37)	670 (52)	NA-OK-KA (9, 53) <sup>a,b</sup>	?
Kuril [Ku]			670 (37)	670 (52)	NA-OK (9) <sup>b</sup>	?
Japan [Jp]			600 (37)	670 (54)	NA-OK (9) <sup>b</sup>	-0.3 (55)
Izu-Bonin [Iz]			600 (37)	670 (56)	PS-IB (57) <sup>a</sup>	?
Mariana [Mr]			650 (37, 58)	670 (56)	PS-MA (7) <sup>a,b</sup>	?

(continued on next page)

Table 1 (continued)

Subduction system	Subduction zone width $\approx$ slab width (km)	Subduction zone edge or slab edge location	Maximum depth extent of seismic slab in upper mantle (km)	Maximum depth extent of tomographic slab in upper mantle (km)	Major overriding plate (+microplate) (+arc block) used to calculate trench velocity	Tectonic accretion (>0) or erosion (<0) (cm/yr)
<i>South America:</i>	7400	N and S				
Colombia [Co]			500 (37, 59)	670 (59)	SA–ND (7, 60) <sup>a</sup>	–0.3 (55, 61)
Peru [Pe]			650 (37, 59)	670 (59)	SA–PE (7, 60) <sup>a</sup>	–0.3 (55, 61)
Bolivia [Bl]			650 (37, 59)	670 (59)	SA–AP (62, 7) <sup>b</sup>	–0.3 (63)
Chile [Ch]			500 (37, 59)	670 (59)	SA–(CH/SC) (7, 16, 60) <sup>a,b</sup>	0.3 (22)
<i>Sunda:</i>	7850 <sup>1</sup>	NW and SE				
(Burma) [Bu]						
Andaman [Ad]			250 (37)	600 (15, 64)	EU–SU–BU (7, 9) <sup>a,b</sup>	0.6 (22)
Sumatra [Sm]			400 (37, 65)	670 (15, 64)	EU–SU (9) <sup>b</sup>	0.2 (22)
Java [Jv]			670 (37, 65)	670 (15, 64)	EU–SU (9) <sup>b</sup>	0.2 (22)
(Banda) [Ba]						

Data for all subduction zones on Earth including (trench–parallel) subduction zone width (which serves as a proxy for slab width) (column 2), slab edge location (column 3), maximum slab tip depth determined from hypocentres (column 4) and tomography (column 5), and kinematic data (overriding plate–microplate–arc block plate circuits (column 6) and accretion/erosion rates (column 7)) used to calculate trench–perpendicular trench migration velocity (Figs. 1 and 2) and toroidal volume fluxes (Table 5) in a number of absolute reference frames. Subduction zone width was primarily calculated from the plate tectonic model of Bird (2003). Note that the Nankai–Ryukyu subduction zone only has one slab edge, as the northeast side of the subduction zone abuts with the northwest Pacific slab. Plate, microplate, and arc block/arc deformation zone abbreviations as plotted in column 6 are indicated by a unique two-letter abbreviation characterised by two capitals and can be found in Table 3. The segments in between brackets in column 1 (Banda, Burma, Dinarides, Hispaniola) are collision zones. In the first column the two-letter unique abbreviation for each subduction zone (capital followed by lower case) is given in between the square brackets. Numbers in parentheses point to the following references: 1—Gutscher et al. (2002); 2—Wortel and Spakman (2000); 3—Rosenbaum and Lister (2004); 4—Ibáñez et al. (1997); 5—Lawver et al. (1995); 6—Kopp et al. (1999), Walpersdorf et al. (1998); 7—Bird (2003); 8—Rangin et al. (1999); 9—Kreemer et al. (2003); 10—Hall and Spakman (2002); 11—Ben—Avraham et al. (1988); 12—McClusky et al. (2000); 13—Lebrun et al. (2000); 14—Livermore (2003); 15—Bijwaard et al. (1998); 16—Thomas et al. (2003), Livermore et al. (1997); 17—Vanneste and Larter (2002); 18—Cooper and Taylor (1987); 19—Tregoning et al. (1998); 20—Quittmeyer (1979); 21—Nilforoushan et al. (2003); 22—Clift and Vannucchi (2004); 23—Bautista et al. (2001); 24—Lallemant et al. (2001); 25—Bostock and VanDecar (1995); 26—Wells et al. (1998); 27—Pérez et al. (1997); 28—van der Hilst and Mann (1994); 29—Papazachos et al. (2000); 30—Eguchi and Uyeda (1983), Nakajima and Hasegawa (2007); 31—Mazzotti et al. (2001); 32—Christova (2004); 33—Nishimura et al. (2004); 34—Feuillet et al. (2002); 35—van der Hilst and Spakman, 1989, VanDecar et al. (2003); 36—Mann et al. (2002); 37—Gudmundsson and Sambridge (1998); 38—Suter et al. (2001); 39—Mercier de Lépinay et al. (1997), Vannucchi et al. (2004); 40—Vannucchi et al. (2001); 41—Bijwaard and Spakman (2000); 42—van der Hilst (1995); 43—Bevis et al. (1995), Zellmer and Taylor (2001); 44—Clift and MacLeod (1999); 45—Wright (1993), Darby and Meertens (1995), Wallace et al., 2004; 46—Reyners et al. (2006); 47—Kennett and Gorbato (2004); 48—Tregoning et al. (1999); 49—Mann and Taira (2004); 50—Taylor et al. (1995), Calmant et al. (1997); 51—Chatelain et al. (1992); 52—van der Hilst et al. (1991); 53—Kozhurin et al. (2006); 54—Kárason and van der Hilst (2000); 55—von Huene and Lallemant (1990); 56—Widiyantoro et al. (1999); 57—Seno et al. (1993); 58—Gvirtzman and Stern (2004); 59—Gutscher et al. (2000); 60—Kley and Monaldi (1998), Dewey and Lamb (1992), Oncken et al., 2006; 61—Clift et al. (2003); 62—Norabuena et al. (1998), Bevis et al. (2001); 63—Laursen et al. (2002); 64—Replumaz et al. (2004); 65—Schöffel and Das (1999). Abbreviations in column one and three: C—central, E—east, N—north, NE—northeast, NW—northwest, S—south, SE—southeast, SW—southwest, W—west.

<sup>a</sup> Based on geological and/or geophysical data.

<sup>b</sup> Based on geodetic measurements.

<sup>c</sup> Geological investigations indicate an overriding plate extensional rate of 2 cm/yr (200 km of extension averaged over the last 10 Myr) (Gutscher et al., 2002), while geodetic investigations indicate a present day extensional rate of only 0.44 cm/yr (Fernandes et al., 2007).

<sup>d</sup> Geological investigations indicate an average overriding plate extensional rate of 6 cm/yr for the last 4 Myr (Rosenbaum and Lister, 2004), while geodetic investigations indicate a present day extensional rate of only 0.2 cm/yr (Serpelloni et al., 2005).

<sup>e</sup> Backarc extension rate based on an average calculated from ~35–50 km of extension from ~1.3–4 Ma to Present as implied by geological investigations (Lawver et al., 1995), while geodetic investigations indicate a present day backarc opening rate of 0.7–0.9 cm/yr (Taylor et al., in review).

<sup>f</sup> Geophysical investigations indicate a trench–perpendicular backarc spreading rate of 3.6–6.7 cm/yr (Thomas et al., 2003), while geodetic investigations indicate a present day trench–perpendicular backarc spreading rate of 4.9–9.1 cm/yr (Smalley et al., 2007).

<sup>g</sup> From this width, ~400 km stems from the westward continuation of the slab below New Guinea (Cooper and Taylor, 1987).

<sup>h</sup> Geological investigations imply a trench–perpendicular overriding plate extensional rate of 0–1.2 cm/yr in the south (Wells et al., 1998), while geodetic investigations indicate a present day trench–perpendicular overriding plate extensional rate of up to 0.6 cm/yr in the south but a shortening rate of up to 0.4 cm/yr in the north (McCaffrey et al., 2007).

<sup>i</sup> From this width, ~800 km stems from the northwestward continuation of the slab below the Dinarides (Wortel and Spakman, 2000).

<sup>j</sup> From this width, ~550 km stems from the westward continuation of the slab below Hispaniola (Mann et al., 2002).

<sup>k</sup> Australia is both the subducting plate and the overriding plate.

<sup>1</sup> From this width, ~1400 km stems from the eastward continuation of the slab below the Banda arc and ~1250 km from the northward continuation of the slab below the Burma arc (Bijwaard et al., 1998; Milson, 2001; Rao and Kalpna, 2005).

Table 2  
Incipient subduction zone data

Incipient subduction zone	Incipient subduction zone width	Maximum depth extent of slab seismicity		Major overriding plate (+microplate) (+arc block) used to calculate trench velocity	Tectonic accretion (>0) or erosion (<0)
	(km)	(km)			(cm/yr)
Negros [Ne]	200	140 (1)		EU–SU–VI (2, 3) <sup>a</sup>	?
Cotobato [Ct]	250	140 (1)		EU–SU–VI (2, 3) <sup>a</sup>	?
Palau [Pl]	250	28 <sup>b</sup>	[62] <sup>c</sup>	PS	?
Hjort [Hj]	250	64 (4)		PA	?
West Sulawesi [Sw]	400	70 (5)	[74] <sup>c</sup>	EU–SU–BS (2, 3) <sup>a</sup>	?
Mussau [Mu]	450	24 <sup>b</sup>	[66] <sup>c</sup>	PA	?
Muertos [Mo]	600	150 (6)		NA–HP (6) <sup>a</sup>	?
Japan Sea [Js]	650	42 <sup>b</sup>	[45] <sup>c</sup>	NA–OK (3) <sup>a</sup>	?
Panama [Pn]	700	66 (7)	[100] <sup>c</sup>	SA–CA–PM (5, 8, 3) <sup>a,d</sup>	?
Yap [Ya]	700	44 <sup>b</sup>	[69] <sup>c</sup>	PS	?
Wetar [We]	1000	30 (9)		AU–TI (5, 3) <sup>a</sup>	?
Philippines [Ph]	1650	150 (1)		EU–SU–VI–(EP/MS/BH) <sup>c</sup> (2, 3) <sup>a</sup>	?
Manus [Ms]	1700	30 <sup>b</sup>	[100] <sup>c</sup>	AU–NB (10) <sup>a</sup>	?
New Guinea [Gu]	1750	128 <sup>b</sup>		AU–(BH/WL) (5, 11) <sup>a</sup>	?

Data for incipient subduction zones on Earth including (trench–parallel) width (column 2), maximum slab tip depth (only determined from hypocentres) (column 3) and kinematic data (overriding plate–microplate–arc block plate circuits (column 5) and accretion/erosion rates (column 6)) used to calculate trench–perpendicular trench migration velocity in a number of absolute reference frames as plotted in Fig. 3. Incipient subduction zone width was primarily calculated from the plate tectonic model of Bird (2003). Plate, microplate, and arc block/arc deformation zone abbreviations as plotted in column 5 are indicated by a unique two-letter abbreviation characterised by two capitals and can be found in Table 3. In the first column the two-letter unique abbreviation for each subduction zone (capital followed by lower case) is given in between the square brackets. Numbers in parentheses point to the following references: 1—Lallemant et al. (1998); 2—Rangin et al. (1999); 3—Kreemer et al. (2003); 4—Meckel et al. (2003); 5—Bird (2003); 6—Mann et al. (2002); 7—Vergara Muñoz (1988); 8—Pérez et al. (2001); 9—McCaffrey (1988); 10—Tregoning et al. (1999); 11—Tregoning et al. (1998).

<sup>a</sup> Based on geodetic measurements.

<sup>b</sup> Determined from the Harvard CMT catalogue (period 1 January 1976 until 1 August 2006).

<sup>c</sup> Numbers in square brackets in column 4 represent estimated thickness of subducting lithosphere based on the age of the lithosphere. These numbers have been used in the calculations in case they exceed the maximum depth extend of seismicity. The  $(age)^{1/2}$  law has been used to estimate the thickness of oceanic lithosphere in the age range of 0 Ma to 80 Ma, with thicknesses increasing from 0 km to 100 km. Oceanic lithosphere with an age exceeding 80 Ma was assigned a 100 km thickness.

<sup>d</sup> Based on geological and/or geophysical data.

<sup>e</sup> EP motion should be incorporated but has not been done in the calculations because rotation parameters for this arc sliver have not yet been determined (Bird, 2003). Motion of MS and BH have not been incorporated either because it is not clear if and where these two entities border the southernmost part of the Philippine trench; due to the complexity of the region, the tectonic setting is uncertain.

as possible (15 out of 28). As such, the calculated data sets are as homogeneous as currently possible.

In the hotspot reference frames, the plate motion relative to the hotspots is averaged for the last 10 Myr (Gordon and Jurdy, 1986; O'Neill et al., 2005), 5.8 Myr (Gripp and Gordon, 2002) or 5.89 Myr (Wessel et al., 2006), while in the no-net-rotation reference frames plate motions are averaged over the last 3 Myr (Argus and Gordon, 1991) or represent current plate motions (i.e. geodetically derived (Kreemer et al., 2003)). The reference frame of Gordon and Jurdy (1986) is based on both Indo-Atlantic and Pacific hotspots, the reference frame of O'Neill et al. (2005) is based exclusively on Indo-Atlantic hotspots, the reference frame of Gripp and Gordon (2002) is primarily based on Pacific hotspots and the reference frame of Wessel et al. (2006) is based exclusively on Pacific hotspots. Trench-directed motion of the overriding plate adds to the amount of trench retreat, while overriding plate motion away from the trench reduces the amount of trench retreat.

Rates are predominantly positive or close to zero in seven reference frames (G&J1986, A&G1991, K2003, H2003+D1994, O2005+D1994, O2005+K2003, W2006+D1994), indicating that the overriding plate is generally moving towards the subducting plate or is close to stationary, as predicted by geodynamic modelling (e.g. Becker and O'Connell, 2001; Conrad and Lithgow-Bertelloni, 2002). Significant negative rates only occur in the reference frame

of Gripp and Gordon (2002). Rates vary significantly between this and the other reference frames (up to ~4 cm/yr), but all trench–perpendicular rates vary between –8.9 and 9.5 cm/yr.

The component of permanent overriding plate trench–perpendicular deformation was compiled from numerous studies in which such rates were determined from geological, geophysical and geodetic investigations (see Table 1). Backarc extension, backarc spreading, intra-arc extension and fore-arc extension add to the amount of trench retreat, because the trench and subduction hinge need to migrate backward (oceanward) to accommodate the extension (Elsasser, 1971; Dewey, 1980; Schellart and Lister, 2004). Overriding plate shortening reduces the amount of trench retreat. For most subduction zones the overriding plate close to the trench is either extending (36.5%) or neutral (45.1%) (Schellart, 2007b). Very high trench–perpendicular backarc spreading rates (7–15 cm/yr) are found in the Southwest Pacific region behind the Tonga, New Hebrides and New Britain arcs. Significant overriding plate shortening is only observed for the Central South America, Japan and Manila subduction zones, and the rates of trench–perpendicular shortening are comparatively small (up to 3 cm/yr).

For a large number of subduction zones, the amount of trench migration has also been corrected for the amount of accretion or erosion of the overriding plate during subduction, as this will also influence migration of the trench and the slab

Table 3  
Two-letter abbreviations for plates, microplates and arc blocks

Plate abbreviation	Plate	Microplate abbreviation	Microplate	Arc block/sliver/deformation zone abbreviation	Arc block/sliver/deformation zone
AN	Antarctica	AM	Amuria	AS	Aegean Sea <sup>a</sup>
AU	Australia	AT	Anatolia	AP	Altiplano
EU	Eurasia	BS	Banda Sea	BE	Betic-Rif <sup>a</sup>
NA	North America	CA	Caribbean	BH	Birds Head
PA	Pacific	MS	Molucca Sea	BU	Burma
PS	Philippine Sea	ND	North Andes	CB	Calabria <sup>a</sup>
SA	South America	NE	Nevada	CH	Chile <sup>a</sup>
		OK	Okhotsk	EP	East Philippines <sup>a</sup>
		SC	Scotia	HP	Hispaniola <sup>a</sup>
		SU	Sunda	IB	Izu-Bonin <sup>a</sup>
		YA	Yangtze	KA	Kamchatka
				KE	Kermadec
				LU	Luzon <sup>a</sup>
				MA	Mariana
				ME	Mexico <sup>a</sup>
				MK	Makran <sup>a</sup>
				NB	North Bismarck
				NH	New Hebrides
				NV	Northern Vancouver Island <sup>a</sup>
				OL	Olympic <sup>a</sup>
				ON	Okinawa
				OR	Oregon <sup>a</sup>
				PE	Peru <sup>a</sup>
				PM	Panama
				SB	South Bismarck
				SL	South Shetland
				SW	Sandwich
				TI	Timor
				TK	Tokai South Kanto <sup>a</sup>
				TO	Tonga
				VI	Visayas <sup>a</sup>
				WL	Woodlark

Abbreviations for plates, microplates, arc blocks, arc slivers and arc deformation zones. Note that these entities are represented with two capitals, following Bird (2003). Newly introduced abbreviations for entities not included in Bird (2003) are NE, BE, CB, CH, EP, HP, IB, LU, ME, MK, NV, OL, OR, PE, TK and VI. Care was taken to make sure these abbreviations were not already assigned previously in Bird (2003) to other entities not discussed in this paper.

<sup>a</sup> Arc slivers and arc deformation zones with relatively diffuse deformation.

(see Table 1). Tectonic accretion has an effect of increasing the amount of retreat due to addition of material to the overriding plate, forcing the subduction hinge to migrate oceanward, whilst tectonic erosion has the opposite effect. Rates of tectonic accretion and erosion vary between  $-0.5$  and  $0.6$  cm/yr and are therefore of subsidiary importance, as these rates are typically an order of magnitude smaller than backarc deformation rates and overriding plate motions. The rates for erosion and accretion have been obtained mostly from the review paper of Cliff and Vannucchi (2004). The most significant tectonic erosion rates have been documented for North Japan ( $-0.3$  cm/yr), northern and central South

America ( $-0.3$  cm/yr), Tonga ( $-0.4$  cm/yr) and Scotia ( $-0.5$  cm/yr). The most significant accretion rates have been documented for southern South America ( $0.3$  cm/yr), Lesser Antilles ( $0.3$  cm/yr), Hellenic ( $0.5$  cm/yr) and Andaman ( $0.6$  cm/yr). Note that, due to a lack of better constraints, the accretion/erosion rate is assumed to be constant with depth along the plate boundary interface.

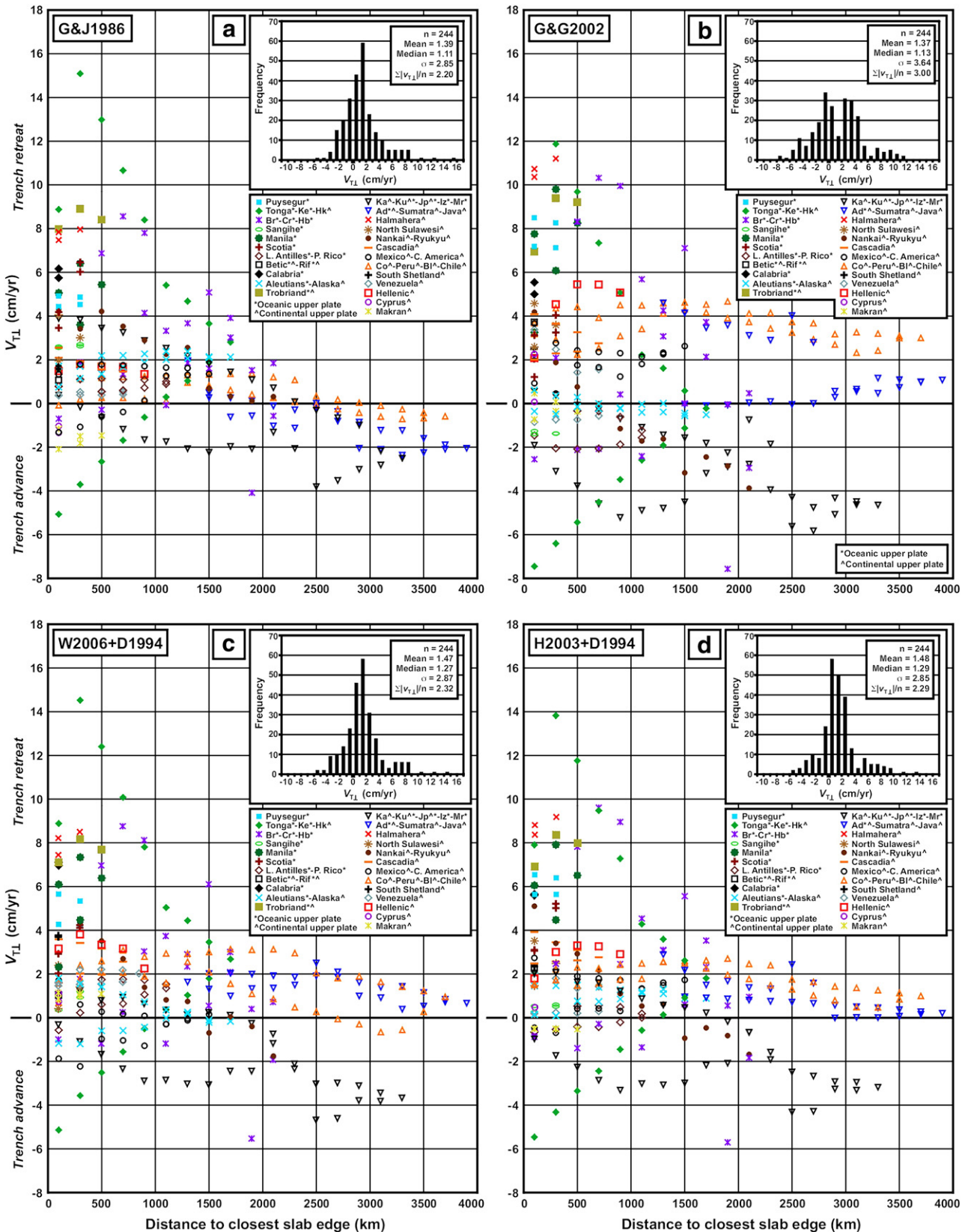
## 2.2. Choice of subduction zones

Subduction zone trench migration was calculated for all the major subduction zones on Earth (Fig. 1). Table 1 summarizes

Fig. 2. Diagrams illustrating the proximity of 200 km wide subduction zone segments to their closest lateral slab edge for all the main subduction zones on Earth and the trench-perpendicular trench migration velocity of these segments in eight global reference frames. (a) Hotspot reference frame of Gordon and Jurdy (1986). (b) Pacific hotspot reference frame of Gripp and Gordon (2002) who use the relative plate motion model of DeMets et al. (1994). (c) Pacific hotspot reference frame of Wessel et al. (2006) combined with the relative plate motion model of DeMets et al. (1994). (d) Antarctic plate reference frame of Hamilton (2003) combined with the relative plate motion model of DeMets et al. (1994). (e) No-net-rotation reference frame of Argus and Gordon (1991) who use the relative plate motion model of DeMets et al. (1990). (f) No-net-rotation reference frame of Kreemer et al. (2003). (g) Indo-Atlantic hotspot reference frame of O'Neill et al. (2005) combined with relative plate motion model of DeMets et al. (1994) (modified from Schellart et al., 2007). (h) Indo-Atlantic hotspot reference frame of O'Neill et al. (2005) combined with relative plate motion model of Kreemer et al. (2003). Positive trench migration velocities indicate trench retreat (i.e. rollback). For details on calculations of data see Methods and Table 1.

the data used to calculate the trench velocities and provides a number of important characteristics for each of these subduction zones, including slab width, maximum depth extent of the

seismic and tomographic slab and parameters used to calculate the trench migration velocity and the toroidal upper mantle volume flux. All subduction zones used in the study show



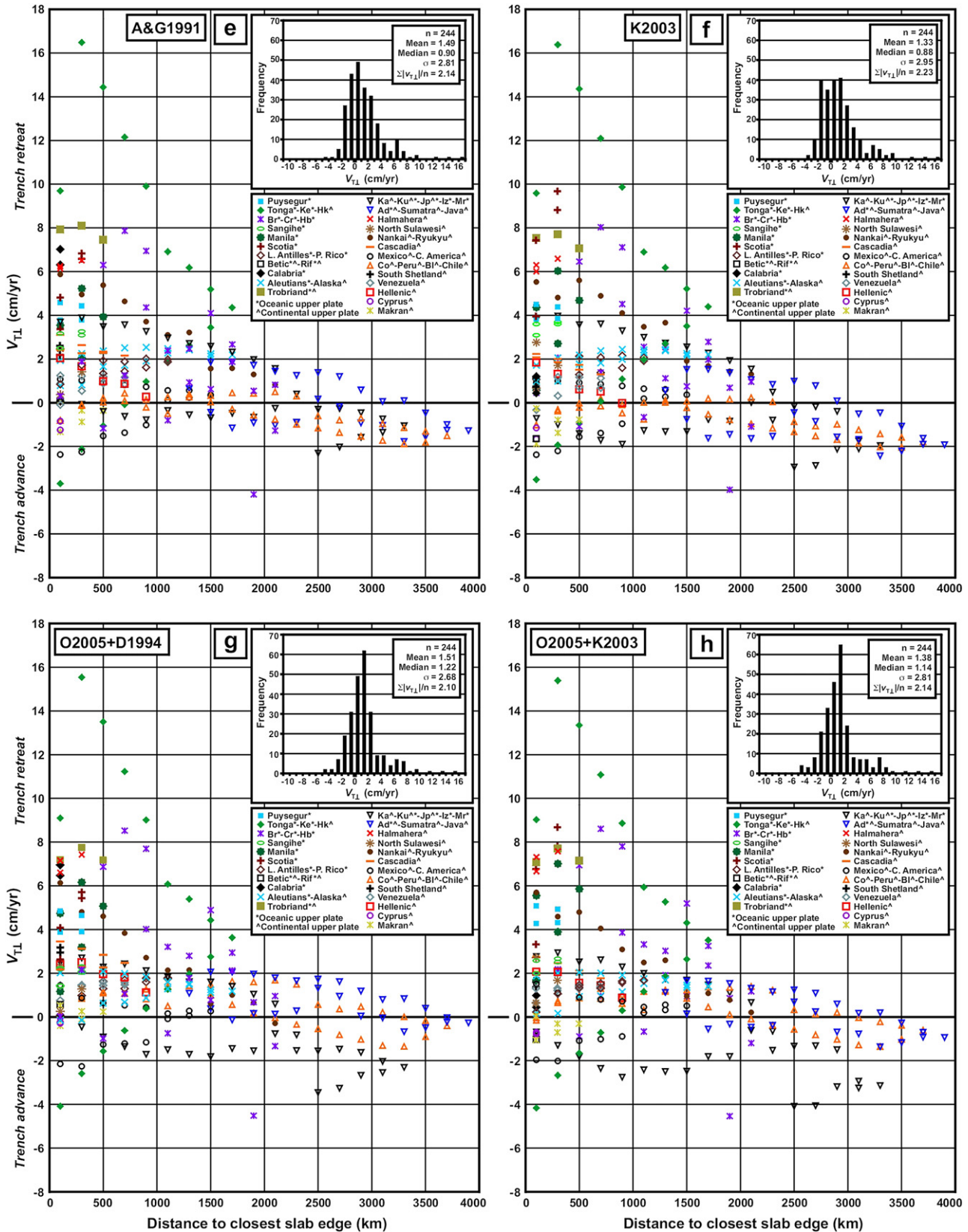


Fig. 2 (continued).

Wadati–Benioff zone seismicity down to a depth of more than 150 km, except Cascadia, Makran, Mexico and South Shetland. Some subduction zones have a poorly developed or relatively short seismic slab (Betic–Rif, Cascadia, Halmahera, Hellenic, Lesser Antilles–Puerto Rico, Makran, Manila, Mexico, parts of South America, South Shetland, Trobriand, and Venezuela). For all of these slabs except South Shetland a distinct and longer slab geometry has been imaged in tomography models (Table 1). All subduction zones have a well-defined trench morphology, except Betic–Rif, Calabria, Cyprus and Hellenic. Finally, all mature subduction zones formed before 5 Ma.

Former subduction zones that are now collision zones, where continental crust or crust from an oceanic plateau is entering the subduction zone, were not taken into account in the trench migration calculations. These include Banda, in which Timor is colliding with the Australian continent, Burma, in which the Burma sliver is colliding with India, Himalaya, where India is colliding with Asia, Seram, in which the arc is colliding with Birds Head, Solomon, in which the arc is colliding with the Ontong–Java Plateau, Hispaniola, where the Bahamas plateau is colliding with the Hispaniola block, Dinarides, where continental crust of the Adriatic promontory is colliding with Eurasia, Carpathians, where the arc has collided with Eurasia, and Apennines, where continental crust of the Adriatic promontory is colliding with Eurasia.

Incipient subduction zones (Table 2) were not included in the trench migration calculations shown in Fig. 2. All incipient subduction zones show Wadati–Benioff zone seismicity to a depth less than ~150 km (except maybe the Philippines) and formed not earlier than 5 Myr ago. For sake of completion, trench migration velocities for these zones have been plotted in a separate figure (Fig. 3). The data used to calculate the trench velocities and additional characteristics of the incipient subduction zones has been plotted in Table 2.

### 2.3. Slab penetration depth and slab width

The slab penetration depth of mature subduction zones was determined from hypocentre locations and seismic tomography models published previously (see Table 1). The longest of either the seismic slab or tomographic slab was used in the calculations. The slab penetration depth for incipient subduction zones was determined only from hypocentre locations (Table 2).

The slab width was calculated primarily from the plate tectonic model of Bird (2003), in which the width of the subduction zone plate boundary (i.e. often coincident with the trench) serves as a proxy for the slab width. A number of subduction systems consist of arc segments that are connected at arc cusps, e.g. Nankai–Ryukyu, Tonga–Kermadec–Hikurangi, New Britain–San Cristobal–New Hebrides (Melanesia), Mexico–Central America, Burma–Andaman–Sumatra–Java–Banda (Sunda), Kamchatka–Kuril–North Japan–Izu–Bonin–Mariana (Northwest Pacific). These systems were determined to consist of one single continuous slab, because the seismic and tomographic signature for each subduction system indicates that the slab is continuous across the individual arc cusps (e.g. Isacks et al., 1968; Yamaoka et al., 1986; Jarrard, 1986; van der

Hilst et al., 1991; Bijwaard et al., 1998; Gudmundsson and Sambridge, 1998; Wortel and Spakman, 2000; Fukao et al., 2001; Kennett and Gorbato, 2004). Obviously, the existence of small slab tears, gaps and slab windows (i.e. with a diameter of <150 km) cannot be ruled out, but these are limited in extent and thus mantle volume fluxes through these openings will be limited in magnitude as well and are negligible compared to the total volume flux generated by the lateral migration of a slab.

A number of subduction zones are connected to collision zones, for which a clear slab geometry is still discernable from focal mechanisms and/or tomography. These slab segments were included in the slab width calculations but not in the volume flux calculations. The Sunda slab continues eastward for ~1400 km as the Banda slab (Bijwaard et al., 1998; Milson, 2001) and northward for ~1250 km as the Burma slab (Bijwaard et al., 1998; Rao and Kalpna, 2005). The Hellenic slab continues northwestward for ~800 km as the Dinarides slab (Wortel and Spakman, 2000). The New Britain and Trobriand slabs both continue westward underneath the New Guinea collision zone for ~400 km (Cooper and Taylor, 1987; Hall and Spakman, 2002). The Lesser Antilles–Puerto Rico slab continues westward for ~550 km as the Hispaniola slab (Mann et al., 2002).

### 2.4. Toroidal volume flux calculations due to lateral slab migration

Subduction of oceanic lithosphere results from two different modes of subduction: (1) trenchward motion of the subducting plate and (2) oceanward retreat of the trench and subduction hinge resulting from rollback of the slab. The first mode is the textbook example of how subduction is commonly perceived. It is described as poloidal mantle flow and can be explained with simple thermal convection models. The second mode is harder to explain as it is associated with both poloidal and toroidal mantle flow. The toroidal component does not directly contribute to the heat loss from the Earth's interior, but is required as a return flow from one side of the slab to the other side to allow for sinking of the slab in the mantle during trench migration. Subduction models have shown that such return flow occurs around the lateral slab edges as a quasi-toroidal-type flow (Kincaid and Griffiths, 2003; Schellart, 2004a; Stegman et al., 2006; Funicello et al., 2006; Schellart, 2008). Recent modelling has also shown that a component of rollback-induced poloidal return flow around the slab tip does not exist (Schellart, 2008). Subduction models have further shown that for relatively narrow slabs ( $\leq 1500$  km) ~70% of the negative buoyancy force of the slab is used to drive this toroidal flow (Schellart, 2004b; Stegman et al., 2006).

The global compilation of trench migration velocities is used to provide a quantitative estimate of the global upper mantle toroidal volume flux ( $\phi_{\text{To}}$ ) associated with this trench migration and lateral slab migration. The upper bound of this flux can be calculated with the following equation:

$$\phi_{\text{To}} = \sum_{s=1}^{s=S} [L(s)|v_{\text{T}\perp}(s)|z_{\text{Slab}}(s)] \quad (2)$$

where  $s$  is the subduction zone segment number,  $S$  is the total number of subduction zone segments,  $L(s)$  is the length of subduction zone segment  $s$ ,  $|v_{T\perp}(s)|$  is the absolute of the trench-perpendicular trench migration velocity of subduction zone segment  $s$ , and  $z_{\text{Slab}}(s)$  is the depth extent of slab segment  $s$ . Since we only consider the volume flux in the upper mantle, the maximum for  $z_{\text{Slab}}(s)$  is 670 km. With Eq. (2) the toroidal flux that is calculated is probably an overestimate of the real

volume flux, since the lithospheric part is included in the calculations. The most conservative estimate would be one in which the thickest of either the subducting plate or overriding plate is excluded in the calculations. The thickest plate will mostly be the subducting plate, because the overriding plate near the subduction zone is mostly thin due to a hot mantle wedge and a high lithospheric thermal gradient (e.g. Currie and Hyndman, 2006). The most practical and logical choice is also

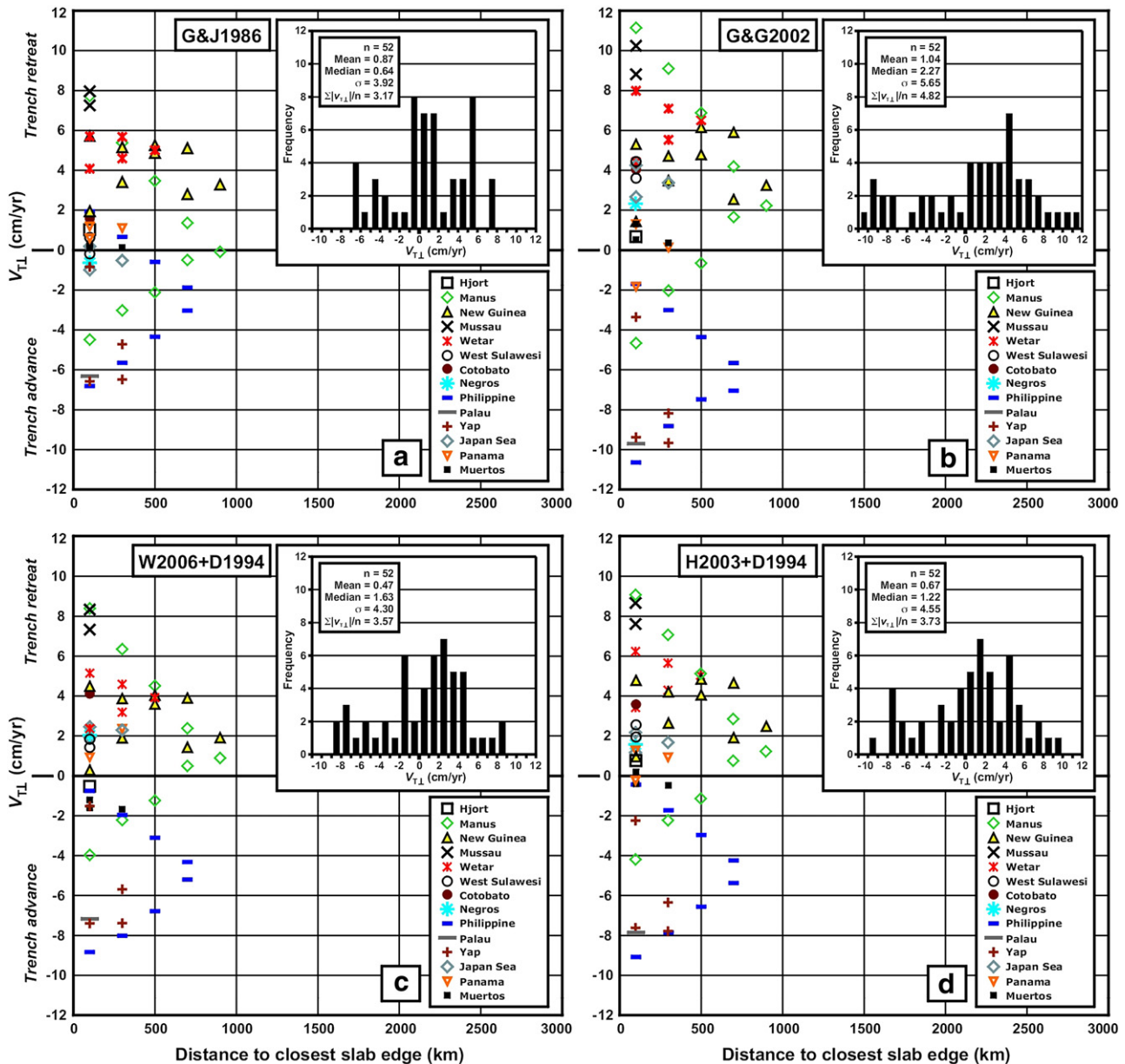


Fig. 3. Diagrams illustrating the proximity of 200 km wide trench segments to their closest lateral edge for all the incipient subduction zones on Earth and the trench-perpendicular trench migration velocity of these segments in eight global reference frames. (a) Hotspot reference frame of Gordon and Jurdy (1986). (b) Pacific hotspot reference frame of Gripp and Gordon (2002) who use the relative plate motion model of DeMets et al. (1994). (c) Pacific hotspot reference frame of Wessel et al. (2006) combined with the relative plate motion model of DeMets et al. (1994). (d) Antarctic plate reference frame of Hamilton (2003) combined with the relative plate motion model of DeMets et al. (1994). (e) No-net-rotation reference frame of Argus and Gordon (1991) who use the relative plate motion model of DeMets et al. (1990). (f) No-net-rotation reference frame of Kreemer et al. (2003). (g) Indo-Atlantic hotspot reference frame of O'Neill et al. (2005) combined with relative plate motion model of DeMets et al. (1994) (modified from Schellart et al., 2007). (h) Indo-Atlantic hotspot reference frame of O'Neill et al. (2005) combined with relative plate motion model of Kreemer et al. (2003). Positive trench migration velocities indicate trench retreat (e.g. rollback). For details on calculations of data see Methods and Table 2.

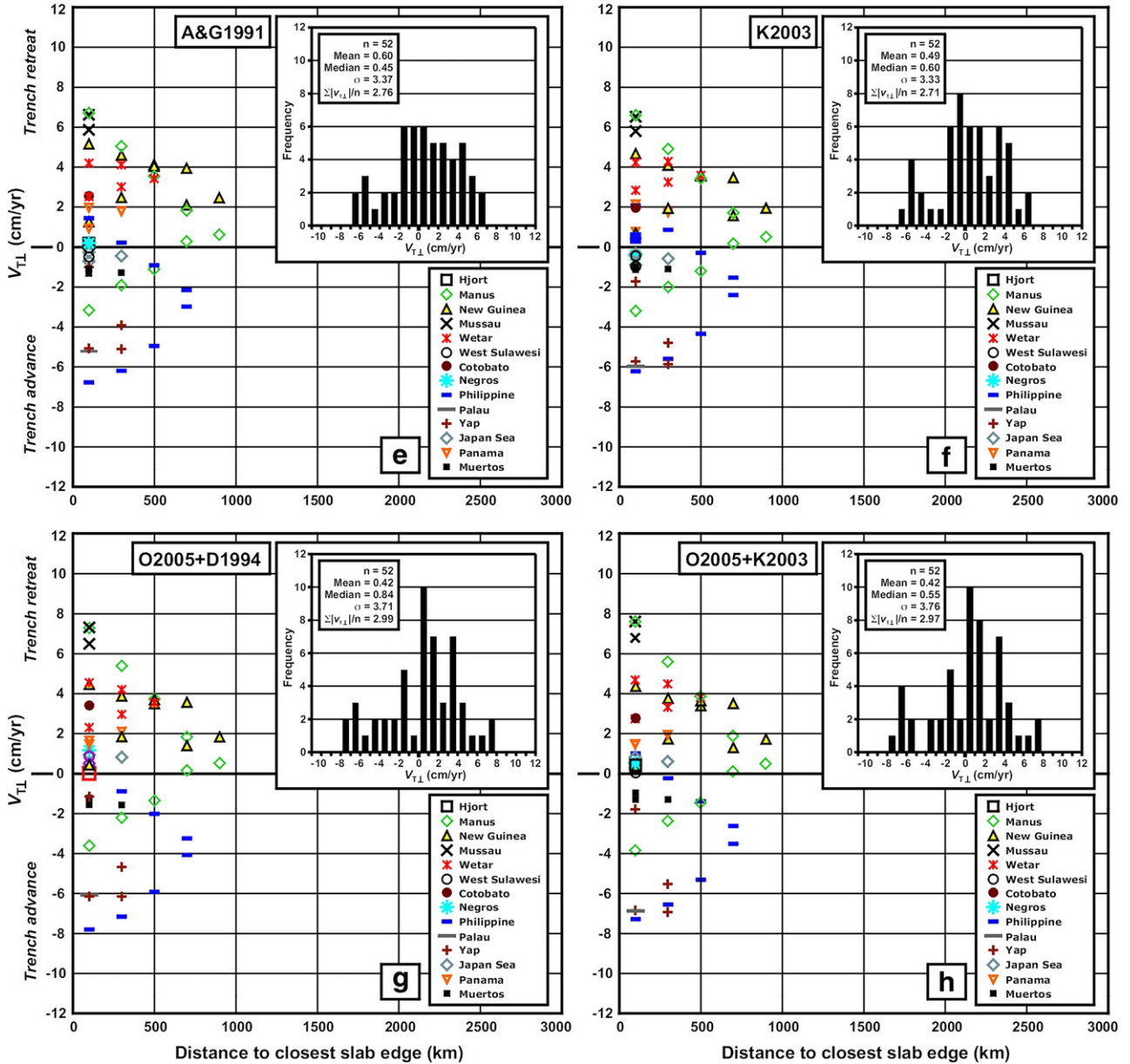


Fig. 3 (continued).

the subducting plate, because the thickness of the subducting plate is best constrained and because, as will be shown in the following sections, trenches predominantly retreat. The most conservative, lower bound, estimate of the volume flux would thus be:

$$\phi_{T_0} = \sum_{s=1}^{s=S} [L(s)|v_{T\perp}(s)|\{z_{\text{Slab}}(s) - z_{\text{SP}}(s)\}] \quad (3)$$

where  $z_{\text{SP}}(s)$  is the depth extent (thickness) of the subducting plate segment  $s$ . With Eqs. (2) and (3) it is assumed that  $|v_{T\perp}|$  is constant with depth, which is not necessarily the case. Indeed, dynamic modelling shows that slabs tend to steepen with time

before the slab tip reaches the transition zone (Funciello et al., 2003; Schellart, 2004a). For such subduction settings, Eq. (2) thus underestimates  $\phi_{T_0}$ . However, in scenarios where the slab tip first starts to interact with the upper–lower mantle transition zone region, trench migration at the surface is often accompanied by slower lateral slab migration near the transition zone. The subduction system only reaches a quasi-steady-state regime of slab draping once the frontal slab part has been draped on top of the transition zone. During this phase  $|v_{T\perp}|$  is approximately constant with depth. In any case, such complexities are extremely hard to quantify and it is thus justified at first to assume that  $|v_{T\perp}|$  is constant with depth. Trench–parallel variation of  $|v_{T\perp}(s)|$ ,  $z_{\text{Slab}}(s)$  and  $z_{\text{SP}}(s)$  has been taken into account.

### 3. Results

#### 3.1. Trench migration velocity

As can be observed in Fig. 2,  $v_{T\perp}$  is predominantly positive or close to zero and the highest retreat velocities are located close to a slab edge in all reference frames. The maximum is observed for the Tonga trench at 300 km from the northern edge. The velocity is significantly smaller at 100 km due to the high obliquity between the strike of the trench and the direction of trench retreat. Such a reduction close to the edge is also observed for some other subduction zones, where the edge of the trench is highly concave towards the mantle wedge side (e.g. southern New Hebrides, Scotia). Such trench curvature is explained by rollback-induced flow around the lateral slab edge, forcing the trench and slab edge to curve in the direction of the mantle return flow, as shown in dynamic models using a variety of slab rheologies (e.g. viscous, Schellart, 2004a; visco-plastic, Schellart et al., 2007; visco-elasto-plastic, Morra et al., 2006). In all reference frames the maximum trench retreat velocity decreases with increasing distance from the closest lateral slab edge. All but three data points from G&G2002 show a retreat velocity  $< 4.0$  cm/yr for distances  $> 2000$  km. When excluding G&G2002, then all retreat velocities, except three data points from H2003 and five data points from W2006, are  $< 2.0$  cm/yr for distances  $> 2000$  km.

In seven out of eight reference frames, the data show a normal distribution with one distinct maximum or a broad maximum in between  $-2$  cm/yr and  $2$  cm/yr and a standard deviation of  $2.68-2.95$ . The data in G&G2002 show two distinct maxima in the frequency plot, one at  $-0.5$  cm/yr and one at  $\sim 3$  cm/yr, and a relatively large standard deviation ( $3.64$ ). G&G2002 also shows a large number (26 data points) of highly negative trench migration velocities (i.e. trench advance) with values in the range  $-8$  to  $-3$  cm/yr. The frequency of highly negative velocities is much smaller in the seven other reference frames ( $2-13$ ).

In all reference frames both trench retreat and trench advance are observed. Trench retreat dominates in all reference frames

with  $61.9-77.9\%$  of all trench segments retreating, the exact number depending on the reference frame (Table 4). Thus, only  $22.1-38.1\%$  of all trench segments are advancing. In regions close to lateral slab edges (i.e. within  $2000$  km of the closest lateral slab edge), trench retreat is even more dominant, with  $75.6-83.4\%$  of the trench segments retreating in seven out of eight reference frames. The mean of  $v_{T\perp}$  is positive in all reference frames (i.e. trench retreat) with values of  $1.33-1.51$  cm/yr. The smallest and largest  $v_{T\perp}$  observed are  $-7.6$  cm/yr (advance) and  $16.5$  cm/yr (retreat). The average of the absolute of  $v_{T\perp}$ ,  $(\sum|v_{T\perp}|)/n$ , is minimum in O2005+D1994 ( $2.10$  cm/yr). All other reference frames have slightly higher values of  $2.14-2.32$  cm/yr, except for G&G2002 with  $(\sum|v_{T\perp}|)/n=3.00$  cm/yr.

Incipient subduction zones show trench velocities varying between  $-10.6$  cm/yr and  $11.1$  cm/yr (Fig. 3). From the 52 trench segments,  $55.8-67.3\%$  is retreating, whilst the remainder is advancing. It is conspicuous that the percentage of advancing incipient subduction zones is larger than for mature subduction zones. Furthermore, the mean trench velocity for incipient subduction zones is significantly smaller ( $v_{T\perp}=0.42-1.04$  cm/yr) than for mature subduction zones ( $1.33-1.51$  cm/yr). Also, incipient subduction zones show both rapid trench retreat and rapid trench advance. Rapid trench advance is nearly absent for the mature subduction zones (Fig. 2).

#### 3.2. Toroidal upper mantle volume flux

In Table 5  $\phi_{T_o}$  has been plotted for both the global set of mature subduction zones and the incipient subduction zones. In all reference frames, the flux from incipient subduction zones constitutes only  $4.4-5.8\%$  (upper bound estimate) and  $1.6-2.2\%$  (lower bound estimate) of the total flux (both mature and incipient subduction zones). The lowest total fluxes of  $569$  km<sup>3</sup>/yr (upper bound estimate) and  $465$  km<sup>3</sup>/yr (lower bound estimate) are found in the Indo-Atlantic hotspot reference frame (O2005+D1994). Fluxes in the other reference frames are slightly higher (up to  $11\%$ ) except in the Pacific hotspot

Table 4  
Tectonic characteristics of different global reference frames

Reference frame	Percentage of retreating trench segments	Percentage of trench segments with $v_{T\perp} > 3.0$ cm/yr	Percentage of trench segments with $v_{T\perp} < -3.0$ cm/yr	Percentage of retreating trench segments for trench segments $< 2000$ km from closest slab edge	$v_{T\perp}$ range for slab segments $> 2000$ km from closest slab edge (cm/yr)	$\sum v_{T\perp} /n$ (cm/yr)
G&J1986	70.5	19.3	2.5	83.4	$-3.80$ to $1.85$	2.18
G&G2002	61.9	33.2	10.7	59.6	$-5.82$ to $4.15$	3.00
W2006+D1994	75.4	20.1	5.3	78.2	$-4.69$ to $3.13$	2.32
H2003+D1994	77.9	17.6	4.9	79.8	$-4.31$ to $2.46$	2.29
A&G1991	68.4	20.5	0.8	79.8	$-2.30$ to $1.57$	2.14
K2003	64.3	20.1	0.8	75.6	$-2.94$ to $1.55$	2.23
O2005+D1994	75.0	16.8	1.6	83.4	$-3.45$ to $1.79$	2.10
O2005+K2003	71.7	16.4	2.9	82.4	$-4.09$ to $1.40$	2.14

Tectonic characteristics for all mature subduction zones (244 trench segments), which were calculated in eight different global references frames (Fig. 2).  $v_{T\perp}$  is trench-perpendicular trench migration velocity (positive indicates trench retreat). Estimated errors for values in columns two, three, four, five, six and seven due to errors in  $v_{T\perp}$  are  $\pm 2\%$ ,  $\pm 1\%$ ,  $\pm 0.5\%$ ,  $\pm 2\%$ ,  $\pm 0.1$  cm/yr and  $\pm 0.1$  cm/yr, respectively. Reference frames: G&J1986 — Gordon and Jurdy (1986); G&G2002 — Gripp and Gordon (2002); W2006+D1994 — Wessel et al. (2006) + DeMets et al. (1994); H2003+D1994 — Hamilton (2003) + DeMets et al. (1994); A&G1991 — Argus and Gordon (1991); K2003 — Kreemer et al. (2003); O2005+D1994 — O'Neill et al. (2005) + DeMets et al. (1994); O2005+K2003 — O'Neill et al. (2005) + Kreemer et al. (2003).

Table 5  
Toroidal volume flux calculations for different global reference frames

Reference frame	$\phi_{To}$ mature subduction zones (upper bound) (km <sup>3</sup> /yr)	$\phi_{To}$ incipient subduction zones (upper bound) (km <sup>3</sup> /yr)	$\phi_{To}$ total (upper bound) (km <sup>3</sup> /yr)	$\phi_{To}$ mature subduction zones (lower bound) (km <sup>3</sup> /yr)	$\phi_{To}$ incipient subduction zones (lower bound) (km <sup>3</sup> /yr)	$\phi_{To}$ total (lower bound) (km <sup>3</sup> /yr)
G&J1986	550.6	29.9	580.5	464.7	9.3	474.0
G&G2002	749.7	45.8	795.6	637.8	13.7	651.5
W2006+D1994	596.8	35.5	632.3	506.4	10.7	517.1
H2003+D1994	576.3	35.8	612.1	489.2	10.9	500.1
A&G1991	543.1	28.0	571.1	457.2	8.8	465.9
K2003	570.7	26.3	596.9	480.5	7.8	488.3
O2005+D1994	538.9	30.2	569.1	455.5	9.2	464.8
O2005+K2003	547.6	28.9	576.5	462.2	8.4	470.6

Upper mantle toroidal volume flux due to lateral slab migration ( $\phi_{To}$ ) for all mature subduction zones (244 trench segments) and incipient subduction zones (52 trench segments) on Earth in eight different global reference frames. Flux is calculated from the upper mantle depth extend of the slab and  $v_{T\perp}$ , which is assumed to be constant throughout the depth of the upper mantle. Flux is calculated with either the entire depth extent of the slab from the Earth’s surface to the slab tip (maximum of 670 km) (columns 2–4, upper bound estimate), or from the base of the subducting lithosphere to the slab tip (maximum of 670 km) (columns 5–7, lower bound estimate). Estimated errors for values in columns two, three, four, five, six and seven due to errors in  $|v_{T\perp}|$  and  $z_{slab}$  are  $\pm 20$  km<sup>3</sup>/yr,  $\pm 2$  km<sup>3</sup>/yr,  $\pm 22$  km<sup>3</sup>/yr,  $\pm 20$  km<sup>3</sup>/yr,  $\pm 2$  km<sup>3</sup>/yr and  $\pm 22$  km<sup>3</sup>/yr, respectively.

reference frame from G&G2002 with a total flux that is significantly higher (40%).

Note that the slab-migration-induced  $\phi_{To}$  will be somewhat higher on Earth than the values presented in Table 5 due to exclusion of toroidal fluxes resulting from lateral migration of slabs that are attached to collision/continental subduction zones (e.g. Banda, Burma, Himalayas, Seram, Solomon, Hispaniola, Dinarides, Carpathians, Apennines). Most importantly, the Banda slab induces a toroidal volume flux of  $\sim 30$  km<sup>3</sup>/yr in all reference frames except G&G2002, in which  $\phi_{To} \approx 60$  km<sup>3</sup>/yr. Himalayas, Seram, Burma and Apennines are also expected to induce a significant toroidal volume flux, each of the order  $10^1$  km<sup>3</sup>/yr owing to relatively fast migration of their plate boundary. However, the values remain speculative due to uncertainty in lateral and depth extent of these slabs and potential slab detachment as illustrated by tomographic models (e.g. Van der Voo et al., 1999; Bijwaard et al., 1998; Wortel and Spakman, 2000). The other collision zone slabs (Solomon, Hispaniola, Dinarides, Carpathians) are expected to induce smaller toroidal volume

fluxes, each of the order  $10^0$  km<sup>3</sup>/yr, owing to relatively slow plate boundary migration, short lateral extend of the slab, short depth extent of the slab, or a combination thereof.

#### 4. Discussion

##### 4.1. Different reference frames

##### 4.1.1. Indo-Atlantic hotspot reference frame as optimal reference frame

Looking at the calculations presented in Tables 4 and 5 it appears that the Indo-Atlantic hotspot reference frame from O’Neill et al. (2005) best meets the four general criteria outlined in the introduction. Indeed, if the eight reference frames are ranked relative to one another for the eight sub-criteria plotted in Tables 4 and 5 (% of retreating trench segments; % of trench segments with  $v_{T\perp} < -3.0$  cm/yr; % of trench segments with  $v_{T\perp} > 3.0$  cm/yr;  $\sum |v_{T\perp}|/n$ ; % of retreating trenches for trench segments located  $< 2000$  km from closest lateral slab edge;  $v_{T\perp}$  range for trench segments  $> 2000$  km from closest lateral slab

Table 6  
Ranking of different global reference frames

Reference frame	% retreating trench segments	% trench segments with $v_{T\perp} > 3.0$ cm/yr	% trench segments with $v_{T\perp} < -3.0$ cm/yr	$\sum  v_{T\perp} /n$	% retreating segments $< 2000$ km from slab edge	$v_{T\perp}$ range for segments $> 2000$ km from slab edge	$\phi_{To}$ total (upper bound)	$\phi_{To}$ total (lower bound)	Total score	Overall ranking
G&J1986	5	4	4	4	1.5	5	4	4	31.5	4
G&G2002	8	8	8	8	8	8	8	8	64	8
W2006+D1994	2	5.5	7	7	6	7	7	7	48.5	7
H2003+D1994	1	3	6	6	4.5	6	6	6	38.5	6
A&G1991	6	7	1.5	2.5	4.5	1	2	2	26.5	3
K2003	7	5.5	1.5	5	7	2	5	5	38	5
O2005+D1994	3	2	3	1	1.5	3	1	1	15.5	1
O2005+K2003	4	1	5	2.5	3	4	3	3	25.5	2

Ranking of the eight global reference frames for eight sub-criteria as plotted in Tables 4 and 5. Note that the lower the score, the better the reference frame meets the eight sub-criteria shown above and the four criteria discussed in the Introduction, and therefore the more likely this reference frame represents an absolute global reference frame. Further note that each category has been weighed equally, which is somewhat arbitrary. This choice is justified, though, considering the lack of knowledge concerning the relative importance of each category.

edge;  $\phi_{T_0}$  total (upper bound);  $\phi_{T_0}$  total (lower bound)), which are deduced from the four general criteria in the introduction, then this reference frame indeed stands out (Table 6). O2005 + D1994 is ranked number 1 with a score of only 15.5 and O2005 + K2003 is ranked number 2 with a score of 25.5. There remains some uncertainty in the ranking, as each of the eight sub-criteria has been equally weighed. As this is a first attempt of ranking different global reference frames such an approach is reasonable.

O2005 + D1994 and O2005 + K2003 are qualitatively and quantitatively rather similar. The difference in upper mantle volume flux is very small, only 1.3% for  $\phi_{T_0}$  total (upper bound) and 1.2% for  $\phi_{T_0}$  total (lower bound). The small difference results to a large extent from the different fluxes for the Manila, Northwest Pacific and South American subduction zones due to different upper plate velocities of the Philippine, Eurasian and South American plates in the relative plate motion model from Kreemer et al. (2003) compared to DeMets et al. (1994).

Apart from being ranked number 1 and 2, there are several geodynamic arguments and predictions from geodynamic models that can be favourable accommodated in the Indo-Atlantic hotspot reference frame.

In particular, in the Indo-Atlantic reference frame, all subducting plates are moving towards their subduction zones in a direction (sub-) perpendicular to the strike of the trench (Fig. 1a). This is even the case for plates for which the subduction zone length makes up only a small percentage of the total circumference of the plate (e.g. Africa, Arabia, Antarctica, South America, Eurasia). Such trenchward motion of the subducting plate is simply explained by slab pull forces, and is in agreement with predictions from geodynamic models of free subduction (e.g. Jacoby, 1973; Zhong and Gurnis, 1995; Schellart, 2004a,b; Enns et al., 2005; Schellart et al., 2007). Plate motion as observed in the Indo-Atlantic hotspot reference frame thus supports the notion that slabs are the main drivers of plate tectonics (e.g. Elsasser, 1971; Forsyth and Uyeda, 1975; Davies, 1999; Bercovici, 2003). In several other reference frames, such trenchward subducting plate motion is less apparent, in particular in the G&G2002 Pacific hotspot reference frame (Fig. 1b).

Furthermore, in the Indo-Atlantic hotspot reference frame, trench migration velocities in the centre of wide subduction zones (i.e. central South America, Sumatra, Japan, San Cristobal) are not only relatively slow (Table 4), the trenchward subducting plate velocities in these regions are always relatively fast (Fig. 1a). Thus, in these central regions, subduction is mostly (75–100%) accommodated by trenchward subducting plate motion. This is in agreement with the result from recent geodynamic modelling, in which subduction in the central regions of wide subduction zones is almost exclusively accommodated by trenchward subducting plate motion, while trench velocities are slow and episodic (see, for example, movie for 6000 km wide slab in Schellart et al., 2007).

Another interesting observation is that in the Indo-Atlantic hotspot reference frame, slabs that penetrate straight through the upper–lower mantle transition zone, as illustrated in cross-sections of mantle tomography models, have relatively slow trench migration velocities. Examples include the Mariana slab (e.g. Widiyantoro et al., 1999) with  $v_{T\perp} \approx -1.8$  to  $-1.7$  cm/yr,

the Central America slab (e.g. Káráson and van der Hilst, 2000) with  $v_{T\perp} \approx -0.1$  to  $0.3$  cm/yr, and the Hellenic slab (e.g. Wortel and Spakman, 2000) with  $v_{T\perp} \approx 2.0$  to  $2.5$  cm/yr. This would be expected, as the high-viscosity lower mantle would partly anchor the lower mantle part of the slab, thereby retarding lateral migration of the upper mantle slab segment and trench migration at the surface. Such slow velocities are also observed in several other reference frames, including both no-net-rotation reference frames. Slow trench migration velocities, however, are not observed in the G&G2002 Pacific hotspot reference frame, with much faster trench migration velocities of  $v_{T\perp} \approx -4.8$  to  $-4.5$  cm/yr for Mariana,  $2.1$  to  $2.3$  cm/yr for Central America, and  $4.5$  to  $5.4$  cm/yr for Hellenic.

As shown in Table 4, trenches in O2005 + D1994 are primarily retreating (75.0%) (71.7% for O2005 + K2003), pointing to rollback of the subducting slab. From the 244 trench segments investigated, only four have significant advancing velocities in the range  $-5.0$  to  $-3.0$  cm/yr (seven in O2005 + K2003). Trench retreat is even more pronounced in regions close to ( $<2000$  km) lateral slab edges, with 83.4% retreating (82.4% in O2005 + K2003). The predominance of trench retreat and the near-absence of rapid trench advance are in agreement with three-dimensional geodynamic models of free subduction, in which trenches predominantly retreat and slabs roll back (Kincaid and Olson, 1987; Schellart, 2004a; Stegman et al., 2006; Funicello et al., 2006). In particular, recent models show that trench retreat close to lateral slab edges is almost invariably regressive, while relatively slow trench advance is only observed to occur episodically in the centre of very wide slabs (Schellart et al., 2007). Trench advance is also observed when a large ( $>10$  cm/yr) trenchward velocity is applied to the subducting plate (Schellart, 2005), or in models with an unrealistically high slab/mantle viscosity ratio (Schellart, 2008).

In conclusion, the results for both O2005 + D1994 and O2005 + K2003 as presented in Tables 4–6 stand out and they are ranked number 1 and 2 respectively. On top of this, there are additional geodynamic arguments and predictions from geodynamic models that can be favourably accommodated in the Indo-Atlantic hotspot reference frame, as discussed above, but not so much in other reference frames, as discussed below. We therefore suggest that plate velocities and plate boundary velocities should be calculated with respect to the Indo-Atlantic hotspot reference frame.

#### 4.1.2. No-net-rotation reference frames

The reference frame that comes out third in the ranking is the no-net-rotation reference frame A&G1991 of Argus and Gordon (1991) (Table 6). Trench segments in this reference frame are also primarily retreating (68.4%). The average of the absolute of  $v_{T\perp}$  is slightly higher than in O2005 + D1994 and the same as in O2005 + K2003, but the central segments of the wide slabs show a smaller range of trench migration velocities (Table 4). The total toroidal volume flux associated with slab migration is nearly identical to the flux in O2005 + D1994 and O2005 + K2003. The no-net-rotation reference frame is based on the geodynamic concept of no-net-torque applied from the plates to the underlying asthenosphere due to plate motion over the

asthenosphere (Argus and Gordon, 1991). The reference frame thus minimizes the global torque (under the assumption of uniform lithosphere–asthenosphere drag and symmetrical plate boundary torques). It is thus encouraging that the no-net-rotation reference frames A&G1991 and K2003 (ranked number 5) come reasonably close to optimising the four criteria outlined in the introduction and the eight sub-criteria in Tables 4 and 5.

However, there are some features of the no-net-rotation reference frames that appear counter-intuitive from a qualitative force balance perspective. For example, one would not expect the South American plate to be moving northward very slowly as observed in K2003 (Fig. 1c) and A&G1991. One would expect it to be moving westward slowly, as it has a mid-ocean ridge that provides a ridge push forcing it westward, it has two westward dipping slabs attached to it, the Scotia slab and the Lesser Antilles slab, which are pulling it westward, and it has a subduction zone along its entire western edge that should apply a suction force. Note that such westward motion is retarded, however, by the subduction hinge of the Nazca slab, as it provides a large resistive force to westward motion of the South American plate. Such resistance is caused by the great width (trench–parallel N–S extent) of the South American subduction zone (Schellart et al., 2007). In any case, relatively slow westward motion of the South American plate would be expected, and is indeed observed in the Indo-Atlantic hotspot reference frame from O'Neill et al. (2005) at rates of 1.5–2 cm/yr.

Thus, it appears that no-net-rotation reference frames contain some elements that are geodynamically unrealistic. Such unrealistic features can be explained by readdressing the basic assumption that underlies the no-net-rotation reference frames, namely the assumption of uniform basal drag. It is generally acknowledged that the lithosphere–asthenosphere drag is not uniform on Earth but varies considerably from place to place. Quantifying such variation is difficult, but one main cause for a non-uniform basal drag is the great variation in lithospheric thickness on Earth, with continental lithosphere mostly thicker than oceanic lithosphere. There are a number of continental cratonic regions (e.g. Scandinavia, Canada, Siberia, Western Australia, West Africa, South Africa) with deep keels down to 200–300 km depth (e.g. Artemieva and Mooney, 2001; Fishwick et al., 2005). Lithosphere with such deep keels below experiences greater resistance to move laterally than oceanic lithosphere with a maximum thickness of ~100 km. Furthermore, temperature estimates below continental lithosphere are close to 1200 °C, but below oceanic lithosphere they are close to 1300 °C (Reston and Phipps Morgan, 2004). Such a temperature variation will affect the viscosity of the asthenosphere and thereby enhance a variation in basal viscous drag below continents and oceans.

#### 4.1.3. Antarctic plate reference frame

The Antarctic plate reference frame H2003+D1994 is ranked number 6 (Table 6) and was proposed to represent an absolute reference frame by Hamilton (2003), because it was argued that the plate is completely surrounded by spreading ridges and should therefore be stationary. As a first-order approximation, the Antarctic plate can indeed be thought of as representing an absolute reference frame. However, the Antarctic plate is not

entirely surrounded by ridges. A small part of its circumference consists of a subduction zone plate boundary, where the Antarctic plate is subducting underneath the southern part of South America. Also, there is no reason to assume that all the transform segments surrounding the Antarctic plate provide an equal resistive force or that all the spreading ridge segments provide an equal push force. In particular, the transform boundary between the Antarctic plate and the Scotia microplate is long and irregular, which could provide a shear traction to the Antarctic plate that is not counter-balanced elsewhere. It is thus likely that the Antarctic plate does move, albeit, most likely, relatively slowly compared to other plates in an absolute reference frame.

If the global trench migration patterns are investigated in the Antarctic reference frame, then a significant number of trench segments are advancing, 42 segments (17.2%) slowly ( $-3.0 < v_{T\perp} < 0.0$  cm/yr) and 12 segments (4.9%) rapidly ( $-6.0 < v_{T\perp} \leq -3.0$  cm/yr). The statement from Hamilton (2003) that all subduction hinges roll back in the Antarctic plate reference frame is thus not supported by the data. In fact, Figs. 1–3 imply that, no matter which reference frame is adopted, there is always a minority of trenches and incipient trenches that advances. It should be added, though, that H2003+D1994 does have the largest percentage of retreating trench segments (77.9%; Table 4).

#### 4.1.4. Pacific hotspot reference frames

The Pacific hotspot reference frame from Gripp and Gordon (2002) G&G2002 is ranked the least favourable (8) of all reference frames. The data in this reference frame (Fig. 2b) are somewhat at odds with the data in all the other reference frames (Fig. 2a,c–h), showing two distinct maxima in the frequency plot instead of a normal distribution as for the other reference frames. G&G2002 also shows the smallest percentage of retreating trench segments (61.9%) and the largest number (26 segments, 10.7%) of fast trench advance velocities with values in the range  $-8.0$  to  $-3.0$  cm/yr. The frequency of highly negative velocities is much smaller in the other reference frames (2–13 segments, 0.8–5.3%). Two-dimensional and three-dimensional geodynamic models of free subduction demonstrate that slabs primarily roll back and trenches primarily retreat (Kincaid and Olson, 1987; Zhong and Gurnis, 1995; Schellart, 2004a; Enns et al., 2005; Stegman et al., 2006; Funicello et al., 2006; Schellart et al., 2007; Schellart, 2008), in disagreement with the results in G&G2002. Models show that relatively slow episodic trench advance occurs in the centre of wide slabs, but  $v_{T\perp}$  ranges only between  $-2.0$  and  $1.0$  cm/yr (Schellart et al., 2007). Velocities in the range  $-8.0$  to  $-3.0$  cm/yr are not observed in these models.

Furthermore, geodynamic models show that slab pull forces pull the trailing subducting plate towards the trench (Jacoby, 1973; Schellart, 2004a,b; Enns et al., 2005; Funicello et al., 2006; Schellart et al., 2007; Schellart, 2008). This is clearly observed in, for example, the Indo-Atlantic hotspot reference frame (Fig. 1a) and the no-net-rotation reference frame (Fig. 1c), but is much less developed in G&G2002 (Fig. 1b). For example, in G&G2002, the African, Antarctic, Arabian,

Juan de Fuca and Cocos plates either move away from their main subduction zone(s) or move towards the subduction zone at a low angle.

The mean of the absolute of the trench–perpendicular trench velocities,  $(\sum |v_{T\perp}|)/n$ , and the toroidal volume flux are highest in G&G2002. It is thus evident that the trench motion in this reference frame maximizes viscous dissipation and is energetically most expensive. As stated by Kaula (1975) flow patterns shift about more slowly than material velocities due to work minimization in a convective fluid. If this is indeed the case then one would conclude that G&G2002 is the least probable “absolute” reference frame. The larger value in this reference frame is in large part due to the rapid trench retreat of the entire South American subduction zone (2–5 cm/yr) and the rapid trench advance of the NW Pacific subduction zone (–6 to 1 cm/yr). Geodynamic modelling has demonstrated that wide slabs migrate relatively slowly, especially in the central region of the subduction zone (Schellart et al., 2007). This is indeed observed in most reference frames (Fig. 2a, c–h, Table 4), but not in G&G2002.

The rate of plate motion in G&G2002 is deduced from the age progression of volcanics of the Hawaiian and Society hotspots on the Pacific plate. One potential problem in using Pacific hotspot reference frames is that it has been demonstrated that the Hawaiian hotspot has experienced large motions with respect to Indo-Atlantic hotspots, the paleomagnetic dipole and the Earth’s spin axis during the Late Cretaceous and Cenozoic (Molnar and Stock, 1987; DiVenere and Kent, 1999; Raymond et al., 2000; Tarduno et al., 2003; Parés and Moore, 2005). Hawaiian hotspot motion is explained by mantle return flow from the northwest Pacific subduction zones towards the East Pacific Rise (Steinberger and O’Connell, 1998). Indeed, the estimated 3.2 cm/yr of ESE-directed motion of the Hawaiian hotspot with respect to the spin axis (Parés and Moore, 2005) accounts for the much larger westward motion of the Pacific plate in G&G2002 with respect to the other reference frames.

An additional complication of the G&G2002 reference frame is that the African plate is moving west to west–southwestward, which would imply that the hotspot tracks on the African plate, such as the Walvis Ridge, would show an age progression in the opposite direction (northeastward) to what is observed (southwestward; Müller et al., 1993). Finally, plate motions described in the Pacific hotspot reference frame cannot account for V-shaped structures of fracture zone segments linking across spreading ridges in the Atlantic Ocean, whilst plate motions in the Indo-Atlantic hotspot reference frame can (Müller and Roest, 1992).

It remains surprising that the rotation parameters from G&G2002 differ substantially from the rotation parameters in the other Pacific hotspot reference frame (W2006+D1994), for which the rotation parameters of the Pacific plate were averaged for an almost equivalent time frame (last 5.8 Myr for G&G2002 and last 5.89 Myr for W2006+D1994). Indeed, the rotation parameters for the Pacific plate are significantly different for G&G2002, with (61.47°N, –89.67°E, –1.06°/Myr), and W2006+D1994, with (58.9°N, –66.83°E, –0.87°/Myr).

#### 4.2. Minimizing viscous dissipation in the upper mantle

The fourth condition from Section 1.2 to find the optimal “absolute” reference frame regards the requirement to minimize viscous dissipation in the mantle by minimizing the toroidal return flow associated with lateral migration of slabs through the upper mantle. Minimizing viscous dissipation by minimizing such return flow has no effect on dissipation at plate boundary faults, such as subduction faults and transform faults, because velocities at these plate boundaries are reference-frame independent and only depend on the relative plate motions.

One could question here, if the minimization of toroidal flow associated with lateral slab migration in the Indo-Atlantic hotspot reference frame also implies that viscous dissipation is minimized for other processes elsewhere in the mantle system. For example, Kaula (1975) argued for a reference frame that is based on minimization of migration of all plate boundaries, including spreading ridges and transform faults. Spreading ridges are here not taken into account, because mantle upwelling below the ridges is only passive (Davies, 1999). Furthermore, spreading ridges are superficial features with gentle slopes at the base of the lithosphere that do not require displacement of significant volumes of mantle material. Transform faults are not taken into account either, because they are also superficial features. Vertical steps of the bottom of the lithosphere across transform faults due to superposition of oceanic lithosphere of different age will only amount to a maximum of a few tens of km for a few transforms with a large offset. Thus, the volumes that need to be displaced due to transform–perpendicular transform fault migration and migration of spreading ridges will be negligible, and so will the associated viscous dissipation, when compared with volume fluxes associated with lateral slab migration.

We expect viscous flow in the lower mantle to be similar in all reference frames, almost exclusively poloidal in nature, and thus viscous dissipations in the lower mantle will be comparable in the different reference frames. The toroidal flow induced by lateral slab migration will be concentrated in the upper mantle, due to the large radial viscosity stratification in the mantle, similar to the toroidal flow induced by the plate motions at the Earth’s surface (i.e. strike–slip motion, oblique subduction and plate spin), which is also confined to the upper mantle (e.g. Ferrachat and Ricard, 1998; Stegman et al., 2002).

One parameter that does require some additional discussion is the lateral migration of continental keels that underlie Archean–Early Proterozoic cratons. Global heat flow investigations and tomographic studies imply that the lithosphere of such cratons has a thickness of 175–350 km, compared to ~100 km thick lithosphere for regions with younger crustal ages (Artemieva and Mooney, 2001; Fishwick et al., 2005). Thus, migration of such cratons will require displacement of significant volumes of upper mantle material. The total volume associated with such migration has been calculated for the eight global reference frames using the global lithospheric thickness map from Artemieva and Mooney (2001). The following eight cratonic regions were incorporated in the calculations, where

Table 7  
Volume fluxes due to continental keel migration in different global reference frames

Reference frame	$\phi_K$ West Africa	$\phi_K$ South Africa	$\phi_K$ Baltic shield–Russian platform	$\phi_K$ Siberia	$\phi_K$ South India	$\phi_K$ West–Central Australia	$\phi_K$ Canadian shield–Greenland	$\phi_K$ Brazilian shield	$\phi_K$ Total
	(km <sup>3</sup> /yr)	(km <sup>3</sup> /yr)	(km <sup>3</sup> /yr)	(km <sup>3</sup> /yr)	(km <sup>3</sup> /yr)	(km <sup>3</sup> /yr)	(km <sup>3</sup> /yr)	(km <sup>3</sup> /yr)	(km <sup>3</sup> /yr)
G&J1986	11.3	1.9	3.7	9.1	5.5	15.4	6.8	2.5	56.1
G&G2002	10.0	0.6	5.3	8.5	4.8	16.2	7.6	9.5	62.4
W2006+D1994	4.4	0.2	3.8	5.4	3.7	12.6	5.9	5.9	41.8
H2003+D1994	6.5	1.1	0.8	1.2	4.7	14.0	8.1	5.7	42.1
A&G1991	17.9	1.9	7.0	10.8	7.4	13.4	8.4	1.6	68.3
K2003	17.4	1.8	7.2	12.6	6.8	12.4	7.7	1.2	67.2
O2005+D1994	12.6	1.1	5.4	6.7	5.5	12.3	7.8	3.4	54.8
O2005+K2003	12.6	1.1	5.5	8.3	5.2	12.1	7.9	3.0	55.7

Upper mantle volume fluxes due to lateral migration of continental keels ( $\phi_K$ ) for the major cratonic shields on Earth in eight different global reference frames. Flux is calculated from the depth extend of the keel with respect to bottom of normal continental lithosphere (~100 km) and the plate velocity component perpendicular to the leading edge of the keel ( $v_{p\perp}$ ). Estimated errors for values in columns two, three, four, five, six, seven, eight, nine and ten due to potential errors in lithospheric thickness are  $\pm 2$  km<sup>3</sup>/yr,  $\pm 0.2$  km<sup>3</sup>/yr,  $\pm 0.5$  km<sup>3</sup>/yr,  $\pm 2$  km<sup>3</sup>/yr,  $\pm 1$  km<sup>3</sup>/yr,  $\pm 6$  km<sup>3</sup>/yr,  $\pm 2$  km<sup>3</sup>/yr,  $\pm 2$  km<sup>3</sup>/yr, and  $\pm 16$  km<sup>3</sup>/yr, respectively.

lithospheric thickness  $\geq 175$  km: Canadian shield, Brazilian shield, Baltic shield–Russian platform, Siberia, West Africa, South Africa, South India and Western–Central Australia.

As can be observed in Table 7, the total volume associated with such keel migration is 42–68 km<sup>3</sup>/yr ( $\pm 16$  km<sup>3</sup>/yr), which is an order of magnitude smaller than that associated with the lateral migration of slabs (Table 5). It should be added here that the potential error in these calculations is rather large ( $\pm 16$  km<sup>3</sup>/yr), because of substantial uncertainty in thickness of the continental keels. This is of particular importance for the fastest continental plate, Australia, where heat flow data suggest that the thickness for Western and Central Australia is only ~175 km (Artemieva and Mooney, 2001), while tomographic investigations suggest it is 200 km and in some places up to 250 km (Fishwick et al., 2005). However, it is clear that the volume flux due to lateral migration of continental keels is of subordinate importance when compared to the volume flux due to migration of slabs through the upper mantle. Nevertheless, it can be observed that O2005+D1994 and O2005+K2003 have the third- and fourth-lowest volume fluxes due to continental keel migration, while that of G&G2002 is substantially higher (Table 7).

#### 4.3. Incipient subduction zones

Incipient subduction zones were not plotted in Fig. 2 but were plotted separately in Fig. 3. Inclusion of the incipient subduction zones in Fig. 2 would not significantly alter the patterns observed in this figure or the conclusions drawn from them. A large number of incipient subduction zones have high trench migration velocities (Fig. 3), but all incipient subduction zones are narrow (<1800 km). Narrow subduction zones would thus not add to the data in the range 1000–3900 km from the slab edge. The trench velocity pattern observed for incipient subduction zones partly agrees with that for mature subduction zones, where rapid trench velocities are also only observed close to slab edges. However, mature subduction zones predominantly show rapid trench retreat, while incipient subduction zones show both rapid trench retreat (e.g. Mussau, New Guinea, Manus) and rapid trench advance (e.g. Yap, Palau, Philippines). This

disparity is explained as such that incipient subduction zones are not yet self-sustaining (Gurnis et al., 2004; Schellart, 2005). Therefore the negative buoyancy force of an incipient slab is small due to the short slab length, and will not drive rapid subduction, trench retreat, and rollback of the slab. The migration of the incipient subduction zones is essentially passive and results predominantly from the motions of the surrounding plates.

#### 4.4. Potential limitations of kinematic models

A number of points have to be kept in mind when interpreting the trends observed in Figs. 2 and 3. In particular, it should be noted that the plate motion relative to some “absolute” reference frame, the global relative plate motion models, the local microplate motions and the overriding plate deformation rates are mostly averaged over different time spans. For example, the Indo-Atlantic hotspot reference frame is averaged over the last 10 Myr and the Pacific hotspot reference frame from Gripp and Gordon (2002) over the last 5.8 Myr, while the no-net-rotation models are based on relative plate motion models that are averaged over the last ~3 Myr (Argus and Gordon, 1991) or the last 10–20 years or so (i.e. geodetically derived, Kreemer et al., 2003). The microplate motions and arc block motions have mostly been derived with geodetic methods, although numerous of these motions have also been derived with geological/geophysical methods, while some have been derived only with geological/geophysical methods. Details are all specified in Tables 1 and 2. The approach is thus, inevitably, not ideal, as one would prefer that all the rotation parameters would be averaged over exactly the same time span, but unfortunately this is not possible (yet?). The data sets that are most homogeneous are K2003 and O2005+K2003, as these models use a geodetic relative plate motion model from Kreemer et al. (2003), while most microplate motions and arc/backarc deformation rates are also geodetically determined (24 out of 28, see Tables 1 and 2).

Nevertheless, acknowledging a degree of in-homogeneity in the data sets, the study does show that for all the eight models the results are essentially the same, with slow trench migration far

from lateral slab edges, fast trench retreat only close to lateral slab edges and predominance of trench retreat, in particular close to lateral slab edges. For example, the results for O2005+D1994, with a geological relative plate motion model and geological  $v_{\text{OPD}\perp}$  rates where possible, and O2005+K2003, with a geodetic relative plate motion model and mostly geodetic  $v_{\text{OPD}\perp}$  rates, are qualitatively and quantitatively very similar (cf. Fig. 2g and h). The same applies to A&G1991 and K2003 (cf. Fig. 2e and f). It is thus concluded that the general results regarding the predominance of trench retreat over trench advance, and the trench migration patterns in relation to slab width and lateral slab edge proximity are solid and robust.

#### 4.5. Previous kinematic studies of trench migration

Global trench migration calculations have been done previously (Garfunkel et al., 1986; Jarrard, 1986; Heuret and Lallemand, 2005; Sdrolias and Müller, 2006), although never at a scale as complete as presented here. In the previous studies, trench migration rates were calculated in only one (Garfunkel et al., 1986; Heuret and Lallemand, 2005; Sdrolias and Müller, 2006) or two global reference frames (Jarrard, 1986). In addition, tectonic accretion/erosion rates were not incorporated in the earlier calculations, although, as stressed before, the influence of such rates is of subordinate importance. Also, these studies, in particular the older ones, mostly excluded motion of microplates, in particular motion for the ones in East Asia, and used a limited number of backarc extension or shortening rates in their calculations. For this reason, trench migration velocities reported here are generally faster than the velocities reported in the older two of the studies cited above.

Garfunkel et al. (1986) presented a novel study of absolute trench velocity calculations for the Sunda subduction zone and the major Pacific subduction zones in a no-net-rotation reference frame from Minster and Jordan (1978). Only two backarc deformation rates were incorporated in the calculations, one for Mariana (5.0 cm/yr) and one for Tonga (3.0 cm/yr). These rates differ from more recent estimates for backarc spreading that have been deduced with geodetic and geophysical methods, with trench-perpendicular backarc opening rates of 6.2–15.0 cm/yr for Tonga (e.g. Bevis et al., 1995; Zellmer and Taylor, 2001) and 0–3.4 cm/yr for Mariana (e.g. Bird, 2003). Trench migration rates in Garfunkel et al. (1986) therefore differ significantly from those reported here. Garfunkel et al. (1986) were one of the first to realize the importance of the global upper mantle volume flux that results from trench migration and lateral slab migration. From their trench migration calculations and slab depth models, a total upper mantle volume flux of 209.8 km<sup>3</sup>/yr was estimated (this was an upper bound estimate as it included the subducting plate thickness). The estimated upper mantle volume flux for the mature subduction zones in this paper is significantly higher for each of the reference frames (538.9–749.7 km<sup>3</sup>/yr (upper bound)) due to inclusion of many additional subduction zones and updated (on average faster) trench migration velocities.

Jarrard (1986) did a comprehensive analysis of subduction zone characteristics including trench migration velocities. The velocities

were calculated in two reference frames, a no-net-rotation reference frame from Minster and Jordan (1978) and a hotspot reference frame from Chase (1978). The analysis included three subduction zones (Palau, Philippines and Yap), which are here considered to be incipient subduction zones (see Section 2.2). This study does include nine additional mature subduction zones and eleven additional incipient subduction zones, which were not considered by Jarrard (1986). Jarrard (1986) only included backarc extension/spreading rates, not shortening rates, and only for Hellenic, Andaman, Kermadec, Tonga, New Hebrides, New Britain, Mariana and Scotia. The study presented here includes many updated backarc deformation rates, and also includes a large number of microplate motions relative to the main overriding plate and backarc deformation rates not incorporated by Jarrard (1986). For this reason, many trench migration velocities reported here differ from those in Jarrard (1986).

Sdrolias and Müller (2006) presented a novel study of absolute trench migration rates for the last 50–60 Myr that were calculated in the Indo-Atlantic hotspot reference frame from O'Neill et al. (2005). Rates were calculated for the Sunda subduction zone and six major subduction zones in the Pacific Ocean (Tonga–Kermadec–Hikurangi, Kuril–Kamchatka–Japan–Izu–Bonin–Mariana, Aleutians–Alaska, Cascadia, Mexico–Central America, South America). For the Present, only the backarc deformation rates behind the Tonga–Kermadec and Mariana subduction zones were incorporated. Motion of a number of microplates (e.g. Amuria, Caribbean, Nevada, North Andes Block, Okhotsk, Scotia, Sunda, Yangtze) and arc blocks (e.g. Altiplano, Burma, Izu–Bonin, Kermadec, Mexico, Oregon, Panama) were not incorporated. This study incorporates seventeen additional subduction zones and includes a large number of microplate and arc block motions in the calculations not incorporated in the study of Sdrolias and Müller (2006). A major advantage of the study from Sdrolias and Müller (2006), however, is that it investigates the trench velocities for the last 50–60 Myr. For this long time span it is evidently very difficult to incorporate the motion of numerous microplates and arc blocks. The research presented here only focusses on the present day trench velocities (averaged over a period that started not earlier than 10 Ma).

Heuret and Lallemand (2005) did a comprehensive global analysis of trench migration velocities for 159 trench segments, each 222 km long, in the hotspot reference frame of Gripp and Gordon (2002). They included a large number of subduction zones in their calculations also investigated here, but did not include Betic–Rif, Calabria, Halmahera, Hellenic, Makran, North Sulawesi, Puysegur, San Cristobal, Sangihe, South Shetland, Trobriand and Venezuela. In addition, they did not do any calculations for the incipient subduction zones. For the subduction zones in East Asia, they took into account motion of the Sunda and Amuria microplates relative to Eurasia, but ignored the relative motions of the Okhotsk and Yangtze microplates (e.g. Kreemer et al., 2003). For the Cascadia subduction zone, they ignored overriding plate deformation as implied by geological and geodetic studies (e.g. Wells et al., 1998; McCaffrey et al., 2007). For the southern segment of the South American subduction zone they ignored motion of the

Scotia microplate relative to South America (e.g. Bird, 2003; Thomas et al., 2003; Smalley et al., 2007). For the Tonga–Kermadec–Hikurangi subduction zone, the authors ignored the motion of the Kermadec arc block relative to the Australian plate, resulting from extension in the Havre Trough and the Taupo volcanic zone (Wright, 1993; Darby and Meertens, 1995; Bird, 2003; Wallace et al., 2004). In addition, the study presented here includes updated rotation parameters published in the last ~ten years for a number of microplates (Scotia, Caribbean, North Andes block) and arc blocks (Andaman, Andes, Kermadec, Mariana, New Hebrides, Panama, Ryukyu, Sandwich, Tokai South Kanto) that were not incorporated in the study of Heuret and Lallemand (2005).

From a qualitative perspective, the results from Heuret and Lallemand (2005) are comparable to the trench migration calculations presented here for the Gripp and Gordon (2002) reference frame. Both show a bimodal distribution for the trench migration velocities (cf. frequency plot in Fig. 2b with Fig. 9b in Heuret and Lallemand (2005)). From a quantitative perspective, the results are rather different, which can be attributed to the differences as described in the previous paragraph. Heuret and Lallemand (2005) drew a general conclusion from their calculations that, on a global scale, trench migration is equally partitioned between trench retreat and trench advance. The current study shows that, by using a more comprehensive set of rotation parameters for plates, microplates and arc blocks and applying this to the same reference frame used by Heuret and Lallemand (2005) (i.e. G&G2002), the equal partitioning between trench retreat and advance breaks down, with 151 retreating trenches (61.9%), 93 advancing trenches (38.1%), and a positive (retreating) mean and median trench velocity of 1.37 cm/yr and 1.13 cm/yr, respectively. The new study also shows that the conclusion from Heuret and Lallemand (2005) is biased due to their adopted reference frame, as all the other reference frames show a larger percentage of retreating trench segments, namely 64.3–77.9% (Fig. 2, Table 4).

#### 4.6. Geodynamic implications and considerations

The global compilation of trench migration patterns for mature and incipient subduction zones provides new insight into the dynamics of subduction, the driving forces of plate tectonics and global mantle convection patterns. First, the study shows that irrespective of the adopted reference frame, trench retreat dominates over trench advance, with 61.9–77.9% of all trenches retreating, that the mean and median trench velocity are always positive (retreating) and that the percentage of rapidly retreating trenches (16.4–33.2% for  $v_{T\perp} > 3.0$  cm/yr) is much greater than the percentage of rapidly advancing trenches (0.8–10.7% for  $v_{T\perp} < -3.0$  cm/yr). This suggests that the negative buoyancy force of the slab plays a dominant role in driving trench migration, because three-dimensional geodynamic simulations of progressive free subduction of negatively buoyant slabs show that trenches and their slabs predominantly retreat (Kincaid and Olson, 1987; Schellart, 2004a,b; Stegman et al., 2006; Funicello et al., 2006; Morra et al., 2006; Schellart et al., 2007; Schellart, 2008).

Geodynamic simulations show that with increasing density contrast between slab and ambient mantle, the trench retreat velocity increases (Schellart, 2004a). However, the great complexity in trench migration patterns observed on Earth and the observation that both old (>100 Ma) oceanic lithosphere can both retreat (e.g. Tonga–Kermadec) and advance (e.g. Japan–Izu–Bonin–Mariana) and young (<50 Ma) oceanic lithosphere can both retreat (e.g. southern New Hebrides, southern Scotia) and advance (e.g. southern Peru, southeastern Central America, Nankai) in all reference frames used in this study (Figs. 1 and 2) implies that the trench migration velocity also depends on other physical parameters.

Geodynamic models have shown and conceptual models have implied that different physical parameters can influence the migration velocity of the trench, subduction hinge and slab. Examples include slab buoyancy (thermal buoyancy, chemical buoyancy, phase changes) (Elsasser, 1971; Vogt, 1973; Molnar and Atwater, 1978; Christensen, 1996; Schellart, 2004a; Schellart and Lister, 2004), overriding plate velocity (Jarrard, 1986; Heuret and Lallemand, 2005), subducting plate velocity (Schellart, 2005), slab to mantle viscosity ratio (Schellart, 2008), slab length (Funicello et al., 2003; Schellart, 2004a, 2005; Stegman et al., 2006) and slab width (Dvorkin et al., 1993; Schellart, 2004a; Stegman et al., 2006; Schellart et al., 2007).

The diagrams in Fig. 2 show that the slab width is a dominant factor in determining the trench migration velocity. In all reference frames rapid trench retreat is only observed close to lateral slab edges. For example, subduction segments that experience rapid trench retreat, such as northern Tonga, southern New Hebrides, southwestern Ryukyu, Calabria, Scotia and New Britain, can all be explained by the close proximity of the trench segments to the closest lateral slab edge, which allows for efficient quasi-toroidal rollback-induced return flow around the lateral slab edge towards the mantle wedge (Schellart et al., 2007). Trench migration far from lateral slab edges (i.e. in the middle of wide, >4000 km, subduction zones) is always relatively slow, such as central South America, Japan–northern Izu–Bonin, central Sunda and San Cristobal. This pattern is very clear in seven of the eight diagrams (Fig. 2a and c–h), and somewhat less clear in Fig. 2b, but this can be attributed to complications of the Pacific hotspot reference frame as discussed in Section 4.1.4.

The diagrams in Fig. 2 show that slab edge proximity is a requirement but does not guarantee rapid trench retreat. This can be attributed to the importance of other parameters in retarding trench migration. The diagrams in Fig. 1a and c also illustrate the importance of slab width regarding the subducting plate velocity. In the central regions of wide subduction zones, the trenchward subducting plate velocity is fast and subduction is accommodated predominantly by trenchward subducting plate motion, not by trench retreat. The results presented in Figs. 1 and 2 thereby agree with the dynamic modelling results presented by Schellart et al. (2007) and confirm the conclusions presented therein.

The general results also show that significant trench advance is rare and can readily be explained by one or more of the following parameters: (1) subduction of buoyant lithosphere

(e.g. aseismic ridges, plateaus, continental crust) (e.g. Vogt, 1973); (2) rapid motion of the overriding plate away from the trench (e.g. Jarrard, 1986; Heuret and Lallemand, 2005); (3) rapid trenchward motion of the subducting plate (e.g. Schellart, 2005); (4) subduction of a wide slab (e.g. Schellart et al., 2007). For example, the Hikurangi subduction segment advances in all reference frames, which can be ascribed primarily due to subduction of the (buoyant) Hikurangi Plateau and Chatham Rise. The Japan–Izu–Bonin–Mariana subduction segment also advances in all reference frames, which can be ascribed to the width of the entire Northwest Pacific subduction zone (6550 km), subduction of the Ogasawara Plateau and Caroline Ridge, the rapid westward motion of the subducting Pacific plate, and the rapid westward motion of the upper Philippine plate. Slow trench advance in the Bolivian orocline and Southern Peru as shown in five out of eight reference frames (Fig. 2a, e–h) can probably be ascribed primarily to the subduction of a wide slab (Schellart et al., 2007) and only partly to the (moderate) trenchward subducting plate velocity. It cannot be ascribed to motion of the overriding South American plate, as it is moving westward to northward in all reference frames, nor can it be ascribed to subduction of the Nazca ridge and Iquique ridge on the subducting Nazca plate, as these are only local features with minor topographic expressions that do not indent the overriding plate as shown in other regions.

## 5. Conclusions

In this paper, the trench migration velocity for all the mature subduction zones and incipient subduction zones on Earth has been calculated in eight different global reference frames. It has been shown that plate velocity and trench velocity can differ substantially between the different reference frames (up to 4 cm/yr). Velocities calculated in the Pacific hotspot reference frame, in particular the one from Gripp and Gordon (2002), differ substantially from those calculated in all the other reference frames, i.e. the Indo-Atlantic hotspot, no-net-rotation and Antarctic plate reference frames. These reference frames show a good agreement for plate and trench velocities. From geodynamic and fluid dynamic considerations and predictions from geodynamic modelling, it was proposed that from the eight reference frames, the best candidate to represent an absolute global reference frame is the one, which optimises the number of trench segments that retreat, minimizes the amount of trench migration in the centre of wide (>4000 km) subduction zones, maximizes the number of retreating trench segments in regions <2000 km from the closest lateral slab edge, minimizes the global average of the absolute of the trench-perpendicular trench migration velocity, and minimizes global viscous dissipation by minimizing the global upper mantle toroidal volume flux that results from lateral slab migration. The calculations presented here and summarized in Tables 4–6 show that these conditions are best met in the Indo-Atlantic hotspot reference frame from O'Neill et al. (2005), either combined with the relative plate motion model from DeMets et al. (1994) (O2005+D1994) or from Kreemer et al. (2003) (O2005+K2003).

Calculations further show that, irrespective of the reference frame, trench retreat always dominates over trench advance, with

61.9–77.9% of the 244 trench segments retreating, that the mean and median trench velocity are always positive (retreating), that fast trench retreat is only found close to lateral slab edges (<1500 km) and that trench retreat is always slow far from slab edges (>2000 km).

The general findings from the calculations are predicted by self-consistent geodynamic models of subduction of dense slabs, in which trenches predominantly retreat. In particular, the results are consistent with the most recent modelling results from Schellart et al. (2007), in which progressive free subduction was modelled in 3D space and was driven by buoyancy forces only. This study focussed on the influence of slab width and lateral slab edge proximity on the trench migration velocity. The calculations in each of the eight reference frames support the hypothesis from Schellart et al. (2007), in which fast trench migration is only found close to lateral slab edges, while trench migration in the centre of wide (>4000 km) subduction zones is always slow. In particular, five of these eight reference frames with the best ranking as presented in Table 6 all show that the fastest trench retreat velocities of 6–17 cm/yr occur within 1500 km of the closest lateral slab edge, while the trench velocities are always <2.0 cm/yr at distances >2000 km from the closest lateral slab edge (Fig. 2a, e–h). The kinematic calculations presented here and previous dynamic modelling studies thus imply that trench motion is primarily driven by the negative buoyancy of the slab with respect to the ambient mantle and is controlled to a large extent by the slab width.

## Acknowledgements

This work benefited from discussions with Ross Griffiths, Virginia Toy, Ross Kerr, Geoff Davies, Thorsten Becker and Dietmar Müller. We would like to thank F. Wallien from *Earth-Science Reviews* for the invitation to write this review paper on subduction and trench migration processes. Comments from Corné Kreemer, Dietmar Müller and an anonymous reviewer on an early version of the paper are greatly appreciated. W.P. Schellart was supported by an APD fellowship and a QE II fellowship from the Australian Research Council, and a J. G. Russell award from the Australian Academy of Science.

## References

- Acton, G.D., Gordon, R.G., 1994. Paleomagnetic tests of Pacific Plate reconstructions and implications for motion between hotspots. *Science* 263, 1246–1254.
- Argus, D.F., Gordon, R.G., 1991. No-net-rotation model of current plate velocities incorporating plate motion model Nuvel-1. *Geophysical Research Letters* 18, 2039–2042.
- Artemieva, I.M., Mooney, W.D., 2001. Thermal thickness and evolution of Precambrian lithosphere: a global study. *Journal of Geophysical Research* 106, 16387–16414.
- Bautista, B.C., Bautista, M.L.P., Oike, K., Wu, F.T., Punongbayan, R.S., 2001. A new insight on the geometry of subducting slabs in northern Luzon, Philippines. *Tectonophysics* 339, 279–310.
- Becker, T.W., O'Connell, J., 2001. Predicting plate velocities with mantle circulation models. *Geochemistry, Geophysics, Geosystems* 2 (2001GC000171).
- Ben-Avraham, Z., Kempler, D., Ginzburg, A., 1988. Plate convergence in the Cyprean arc. *Tectonophysics* 146, 231–240.
- Bercovici, D., 2003. The generation of plate tectonics from mantle convection. *Earth and Planetary Science Letters* 205, 107–121.

- Bevis, M., et al., 2001. On the strength of interplate coupling and the rate of back arc convergence in the Central Andes: an analysis of the interseismic velocity field. *Geochemistry, Geophysics, Geosystems* 2 (2001GC000198).
- Bevis, M., et al., 1995. Geodetic observations of very rapid convergence and back-arc extension at the Tonga Arc. *Nature* 374, 249–251.
- Bijwaard, H., Spakman, W., 2000. Non-linear global P-wave tomography by iterated linearized inversion. *Geophysical Journal International* 141, 71–82.
- Bijwaard, H., Spakman, W., Engdahl, E.R., 1998. Closing the gap between regional and global travel time tomography. *Journal of Geophysical Research* 103, 30055–30078.
- Bird, P., 2003. An updated digital model of plate boundaries. *Geochemistry, Geophysics, Geosystems* 4, 1027. doi:10.1029/2001GC000252.
- Bostock, M.G., VanDecar, J.C., 1995. Upper mantle structure of the northern Cascadia subduction zone. *Canadian Journal of Earth Sciences* 32, 1–12.
- Buiter, S.J.H., Govers, R., Wortel, M.J.R., 2001. A modelling study of vertical surface displacements at convergent plate margins. *Geophysical Journal International* 147, 415–427.
- Calmant, S., et al., 1997. Interseismic and coseismic motions in GPS series related to the M (sub s) 7.3 July 13, 1994, Malekula earthquake, central New Hebrides subduction zone. *Geophysical Research Letters* 24, 3077–3080.
- Chase, C.G., 1978. Plate kinematics: The Americas, East Africa, and the rest of the world. *Earth and Planetary Science Letters* 37, 355–368.
- Chatelain, J.-L., Molnar, P., Prévot, R., Isacks, B., 1992. Detachment of part of the downgoing slab and uplift of the New Hebrides (Vanuatu) Islands. *Geophysical Research Letters* 19, 1507–1510.
- Christensen, U.R., 1996. The influence of trench migration on slab penetration into the lower mantle. *Earth and Planetary Science Letters* 140, 27–39.
- Christova, C., 2004. Stress field in the Ryukyu–Kyushu Wadati–Benioff zone by inversion of earthquake focal mechanisms. *Tectonophysics* 384, 175–189.
- Clift, P.D., MacLeod, C.J., 1999. Slow rates of subduction erosion estimated from subsidence and tilting of the Tonga forearc. *Geology* 27, 411–414.
- Clift, P., Vannucchi, P., 2004. Controls on tectonic accretion versus erosion in subduction zones: implications for the origin and recycling of the continental crust. *Reviews of Geophysics* 42, RG2001. doi:10.1029/2003RG000127.
- Clift, P.D., Pecher, I., Kukowski, N., Hampel, A., 2003. Tectonic erosion of the Peruvian forearc, Lima Basin, by subduction and Nazca Ridge collision. *Tectonics* 22, 1023. doi:10.1029/2002TC001386.
- Conrad, C.P., Lithgow-Bertelloni, C., 2002. How mantle slabs drive plate tectonics. *Science* 298, 207–209.
- Cooper, P., Taylor, B., 1987. Seismotectonics of New Guinea; a model for arc reversal following arc–continent collision. *Tectonics* 6, 53–67.
- Currie, C.A., Hyndman, R.D., 2006. The thermal structure of subduction zone back arcs. *Journal of Geophysical Research* 111, B08404. doi:10.1029/2005JB004024.
- Darby, D.J., Meertens, C.M., 1995. Terrestrial and GPS measurements of deformation across the Taupo back arc and Hikurangi forearc regions in New Zealand. *Journal of Geophysical Research* 100, 8221–8232.
- Davies, G.F., 1999. *Dynamic Earth: Plates, Plumes and Mantle Convection*. Cambridge University Press, Cambridge. 460 pp.
- DeMets, C., Gordon, R.G., Argus, D.F., Stein, S., 1990. Current plate motions. *Geophysical Journal International* 101, 425–478.
- DeMets, C., Gordon, R.G., Argus, D.F., Stein, S., 1994. Effect of recent revisions to the geomagnetic reversal time scale on estimates of current plate motions. *Geophysical Research Letters* 21, 2191–2194.
- Dewey, J.F., 1980. Episodicity, sequence, and style at convergent plate boundaries. In: Strangway, D.W. (Ed.), *The continental crust and its mineral deposits*. Special Paper–Geological Association of Canada, Toronto, ON, Canada, pp. 553–573.
- Dewey, J.F., Lamb, S.H., 1992. Active tectonics of the Andes. *Tectonophysics* 205, 79–95.
- DiVenere, V., Kent, D.V., 1999. Are the Pacific and Indo-Atlantic hotspots fixed? Testing the plate circuit through Antarctica. *Earth and Planetary Science Letters* 170, 105–117.
- Duncan, R.A., 1981. Hotspots in the southern oceans—an absolute frame of reference for motion of the gondwana continents. *Tectonophysics* 74, 29–42.
- Dvorkin, J., Nur, A., Mavko, G., Ben-Avraham, Z., 1993. Narrow subducting slabs and the origin of backarc basins. *Tectonophysics* 227, 63–79.
- Eguchi, T., Uyeda, S., 1983. Seismotectonics of the Okinawa Trough and Ryukyu Arc. *Chung Kuo Ti Ch'ih Hsueh Hui Chuan Kan*=Memoir of the Geological Society of China 5, 189–210.
- Elsasser, W.M., 1971. Sea-floor spreading as thermal convection. *Journal of Geophysical Research* 76, 1101–1112.
- Enns, A., Becker, T.W., Schmeling, H., 2005. The dynamics of subduction and trench migration for viscosity stratification. *Geophysical Journal International* 160, 761–775.
- Fernandes, R.M.S., et al., 2007. Surface velocity field of the Ibero–Maghrebian segment of the Eurasia–Nubia plate boundary. *Geophysical Journal International* 169, 315–324.
- Ferrachat, S., Ricard, Y., 1998. Regular vs. chaotic mantle mixing. *Earth and Planetary Science Letters* 155, 75–86.
- Feuillet, N., Manighetti, I., Tapponnier, P., Jacques, E., 2002. Arc parallel extension and localization of volcanic complexes in Guadeloupe, Lesser Antilles. *Journal of Geophysical Research* 107, 2331. doi:10.1029/2001JB000308.
- Fishwick, S., Kennett, B.L.N., Reading, A.M., 2005. Contrasts in lithospheric structure within the Australian craton—insights from surface wave tomography. *Earth and Planetary Science Letters* 231, 163–176.
- Forsyth, D.W., Uyeda, S., 1975. On the relative importance of the driving forces of plate motion. *The Geophysical Journal of the Royal Astronomical Society* 43, 163–200.
- Fukao, Y., Widiyantoro, S., Obayashi, M., 2001. Stagnant slabs in the upper and lower mantle transition region. *Reviews of Geophysics* 39, 291–323.
- Funciello, F., Faccenna, C., Giardini, D., Regenauer-Lieb, K., 2003. Dynamics of retreating slabs (part 2): insights from 3-D laboratory experiments. *Journal of Geophysical Research* 108 (B4), 2207. doi:10.1029/2001JB000896.
- Funciello, F., et al., 2006. Mapping mantle flow during retreating subduction: laboratory models analyzed by feature tracking. *Journal of Geophysical Research* 111, B03402. doi:10.1029/2005JB003792.
- Garfunkel, Z., Anderson, C.A., Schubert, G., 1986. Mantle circulation and the lateral migration of subducted slabs. *Journal of Geophysical Research* 91, 7205–7223.
- Gordon, R.G., Jurdy, D.M., 1986. Cenozoic global plate motions. *Journal of Geophysical Research* 91, 12389–12406.
- Gripp, A.E., Gordon, R.G., 1990. Current plate velocities relative to the hotspots incorporating the Nuvel-1 global plate motion model. *Geophysical Research Letters* 17, 1109–1112.
- Gripp, A.E., Gordon, R.G., 2002. Young tracks of hotspots and current plate velocities. *Geophysical Journal International* 150, 321–361.
- Gudmundsson, O., Sambridge, M.J., 1998. A regionalized upper mantle (RUM) seismic model. *Journal of Geophysical Research* 103, 7121–7136.
- Gurnis, M., Hall, C., Lavier, L., 2004. Evolving force balance during incipient subduction. *Geochemistry, Geophysics, Geosystems* 5, Q07001. doi:10.1029/2003GC000681.
- Gutscher, M.A., Spakman, W., Bijwaard, H., Engdahl, E.R., 2000. Geodynamics of flat subduction: seismicity and tomographic constraints from the Andean margin. *Tectonics* 19, 814–833.
- Gutscher, M.-A., et al., 2002. Evidence for active subduction beneath Gibraltar. *Geology* 30, 1071–1074.
- Gvirtzman, Z., Stern, R.J., 2004. Bathymetry of Mariana trench–arc system and formation of the Challenger Deep as a consequence of weak plate coupling. *Tectonics* 23, TC2011. doi:10.1029/2003TC001581.
- Hall, R., Spakman, W., 2002. Subducted slabs beneath the eastern Indonesia–Tonga region; insights from tomography. *Earth and Planetary Science Letters* 201, 321–336.
- Hamilton, W.B., 2003. An alternative Earth. *GSA Today* 13 (11), 4–12.
- Heuret, A., Lallemand, S., 2005. Plate motions, slab dynamics and back-arc deformation. *Physics of the Earth and Planetary Interiors* 149, 31–51.
- Ibáñez, J.M., et al., 1997. Intermediate-focus earthquakes under South Shetland Islands (Antarctica). *Geophysical Research Letters* 24, 531–534.
- Isacks, B., Oliver, J., Sykes, L.R., 1968. Seismology and the new global tectonics. *Journal of Geophysical Research* 73, 5855–5899.
- Jacoby, W.R., 1973. Model experiment of plate movements. *Nature (Physical Science)* 242, 130–134.

- Jarrard, R.D., 1986. Relations among subduction parameters. *Reviews of Geophysics* 24, 217–284.
- Károni, H., van der Hilst, R.D., 2000. Constraints on mantle convection from seismic tomography. In: Richards, M.A., Gordon, R.G., van der Hilst, R.D. (Eds.), *The History and Dynamics of Global Plate Motions*. Geophysical Monograph, pp. 277–288.
- Kaula, W.M., 1975. Absolute plate motions by boundary velocity minimizations. *Journal of Geophysical Research* 80, 244–248.
- Kennett, B.L.N., Gorbato, A., 2004. Seismic heterogeneity in the mantle—strong shear wave signature of slabs from joint tomography. *Physics of the Earth and Planetary Interiors* 146, 87–100.
- Kincaid, C., Griffiths, R.W., 2003. Laboratory models of the thermal evolution of the mantle during rollback subduction. *Nature* 425, 58–62.
- Kincaid, C., Olson, P., 1987. An experimental study of subduction and slab migration. *Journal of Geophysical Research* 92, 13832–13840.
- Kley, J., Monaldi, C.R., 1998. Tectonic shortening and crustal thickness in the Central Andes: how good is the correlation? *Geology* 26, 723–726.
- Kopp, C., Flueh, E.R., Neben, S., 1999. Rupture and accretion of the Celebes Sea crust related to the North-Sulawesi subduction: combined interpretation of reflection and refraction seismic measurements. *Journal of Geodynamics* 27, 309–325.
- Koppers, A.P., Morgan, J.P., Morgan, J.W., Staudigel, H., 2001. Testing the fixed hotspot hypothesis using <sup>40</sup>Ar/<sup>39</sup>Ar age progressions along seamount trails. *Earth and Planetary Science Letters* 185, 237–252.
- Kozhurin, A., et al., 2006. Trenching studies of active faults in Kamchatka, eastern Russia: Palaeoseismic, tectonic and hazard implications. *Tectonophysics* 417, 285–304.
- Kremer, C., Holt, W.E., 2001. A no-net-rotation model of present-day surface motions. *Geophysical Research Letters* 28, 4407–4410.
- Kremer, C., Holt, W.E., Haines, A.J., 2003. An integrated global model of present-day plate motions and plate boundary deformation. *Geophysical Journal International* 154, 8–34.
- Lallemant, S.E., et al., 1998. Genetic relations between the central and southern Philippine Trench and the Sangihe Trench. *Journal of Geophysical Research* 103, 933–950.
- Lallemant, S., Font, Y., Bijwaard, H., Kao, H., 2001. New insights on 3-D plates interaction near Taiwan from tomography and tectonic implications. *Tectonophysics* 335, 229–253.
- Laursen, J., Scholl, D.W., von Huene, R., 2002. Neotectonic deformation of the central Chile margin: deepwater forearc basin formation in response to hot spot ridge and seamount subduction. *Tectonics* 21, 1038. doi:10.1029/2001TC901023.
- Lawver, L.A., Keller, R.A., Fisk, M.R., Strelin, J.A., 1995. Bransfield Strait, Antarctic Peninsula, active extension behind a dead arc. In: Taylor, B. (Ed.), *Backarc basins: tectonics and magmatism*. Plenum Press, New York, pp. 315–342.
- Lebrun, J.-F., Lamarche, G., Collet, J.-Y., Delteil, J., 2000. Abrupt strike–slip fault to subduction transition: the Alpine fault–Puysegur trench connection, New Zealand. *Tectonics* 19, 688–706.
- Livermore, R.A., 2003. Back-arc spreading and mantle flow in the East Scotia Sea. In: Larter, R.D., Leat, P.T. (Eds.), *Intra-oceanic Subduction Systems: Tectonic and Magmatic Processes*. Geological Society, London, Special Publications, pp. 315–331.
- Livermore, R., Cunningham, A., Vanneste, L., Larter, R.D., 1997. Subduction influence on magma supply at the East Scotia Ridge. *Earth and Planetary Science Letters* 150, 261–275.
- Mann, P., Taira, A., 2004. Global tectonic significance of the Solomon Islands and Ontong Java Plateau convergent zone. *Tectonophysics* 389, 137–190.
- Mann, P., et al., 2002. Oblique collision in the northeastern Caribbean from GPS measurements and geological observations. *Tectonics* 21, 1057. doi:10.1029/2001TC001304.
- Mazzotti, S., Henry, P., Le Pichon, X., 2001. Transient and permanent deformation of central Japan estimated by GPS 2. Strain partitioning and arc–arc collision. *Earth and Planetary Science Letters* 184, 455–469.
- McCaffrey, R., 1988. Active tectonics of the eastern Sunda and Banda arcs. *Journal of Geophysical Research* 93, 15163–15182.
- McCaffrey, R., et al., 2007. Fault locking, block rotation and crustal deformation in the Pacific northwest. *Geophysical Journal International* 169, 1315–1340.
- McClusky, S., et al., 2000. Global positioning system constraints on plate kinematics and dynamics in the eastern Mediterranean and Caucasus. *Journal of Geophysical Research* 105, 5695–5719.
- Meckel, T.A., et al., 2003. Underthrusting at the Hjort Trench, Australian–Pacific plate boundary: incipient subduction? *Geochemistry, Geophysics, Geosystems* 4, 1099. doi:10.1029/2002GC000498.
- Mercier de Lépinay, B., et al., 1997. Large Neogene subsidence event along the Middle Andes Trench off Mexico (18°N–19°N): evidence from submersible observations. *Geology* 25, 387–390.
- Milson, J., 2001. Subduction in Eastern Indonesia: how many slabs? *Tectonophysics* 338, 167–178.
- Minster, J.B., Jordan, T.H., 1974. Numerical modelling of instantaneous plate tectonics. *Geophysical Journal of the Royal Astronomical Society* 36, 541–576.
- Minster, J.B., Jordan, T.H., 1978. Present-day plate motions. *Journal of Geophysical Research* 83, 5331–5354.
- Molnar, P., Atwater, T., 1978. Interarc spreading and Cordilleran tectonics as alternates related to the age of subducted oceanic lithosphere. *Earth and Planetary Science Letters* 41, 330–340.
- Molnar, P., Stock, J., 1987. Relative motions of hotspots in the Pacific, Atlantic and Indian oceans since Late Cretaceous time. *Nature* 327, 587–591.
- Morgan, W.J., 1971. Convection plumes in the lower mantle. *Nature* 230, 42–43.
- Morra, G., Regenauer-Lieb, K., Giardini, D., 2006. Curvature of oceanic arcs. *Geology* 34, 877–880.
- Müller, R.D., Roest, W.R., 1992. Fracture zones in the North Atlantic from combined Geosat and Seasat data. *Journal of Geophysical Research* 97, 3337–3350.
- Müller, R.D., Royer, J.-Y., Lawver, L.A., 1993. Revised plate motions relative to the hotspots from combined Atlantic and Indian Ocean hotspot tracks. *Geology* 21, 275–278.
- Nakajima, J., Hasegawa, A., 2007. Subduction of the Philippine Sea plate beneath southwestern Japan: slab geometry and its relationship to arc magmatism. *Journal of Geophysical Research* 112, B08306. doi:10.1029/2006JB004770.
- Nilforoushan, F., et al., 2003. GPS network monitors the Arabia–Eurasia collision deformation in Iran. *Journal of Geodesy* 77, 411–422.
- Nishimura, S., Hashimoto, M., Ando, M., 2004. A rigid block rotation model for the GPS derived velocity field along the Ryukyu arc. *Physics of the Earth and Planetary Interiors* 142, 185–203.
- Norabuena, E., et al., 1998. Space geodetic observations of Nazca–South America convergence across the Central Andes. *Science* 279, 358–362.
- O’Neill, C., Müller, D., Steinberger, B., 2005. On the uncertainties in hot spot reconstructions and the significance of moving hot spot reference frames. *Geochemistry, Geophysics, Geosystems* 6, Q04003. doi:10.1029/2004GC000784.
- Oncken, O., et al., 2006. Deformation of the Central Andean upper plate system—facts, fiction, and constraints for plateau models. In: Oncken, O., et al. (Ed.), *The Andes-Active Subduction Orogeny*. Springer, pp. 3–27.
- Papazachos, B.C., Karakostas, V.G., Papazachos, C.B., Scordilis, E.M., 2000. The geometry of the Wadati–Benioff zone and lithospheric kinematics in the Hellenic arc. *Tectonophysics* 319, 275–300.
- Parés, J.M., Moore, T.C., 2005. New evidence for the Hawaiian hotspot plume motion since the Eocene. *Earth and Planetary Science Letters* 237, 951–959.
- Pérez, O.J., Jaimes, M.A., Garcia, E., 1997. Microseismicity evidence for subduction of the Caribbean plate beneath the South American plate in northwestern Venezuela. *Journal of Geophysical Research* 102, 17875–17882.
- Pérez, O.J., et al., 2001. Velocity field across the southern Caribbean plate boundary and estimates of Caribbean/South-American plate motion using GPS geodesy 1994–2000. *Geophysical Research Letters* 28, 2987–2990.
- Quittmeyer, R.C., 1979. Seismicity variations in the Makran region of Pakistan and Iran; relation to great earthquakes. *Pure and Applied Geophysics* 117, 1212–1228.
- Rangin, C., et al., 1999. Plate convergence measured by GPS across the Sundaland/Philippine Sea Plate deformed boundary: the Philippines and eastern Indonesia. *Geophysical Journal International* 139, 296–316.

- Rao, N.P., Kalpna, 2005. Deformation of the subducted Indian lithospheric slab in the Burmese arc. *Geophysical Research Letters* 32, L05301. doi:10.1029/2004GL022034.
- Raymond, C.A., Stock, J.M., Cande, S.C., 2000. Fast Paleogene motion of the Pacific hotspots from revised global plate circuit constraints. In: Richards, M.A., Gordon, R.G., van der Hilst, R.D. (Eds.), *The History and Dynamics of Global Plate Motions*. Geophysical Monograph. American Geophysical Union, pp. 359–375.
- Replumaz, A., Káráson, H., van der Hilst, R.D., Besse, J., Tapponnier, P., 2004. 4-D evolution of SE Asia's mantle from geological reconstructions and seismic tomography. *Earth and Planetary Science Letters* 221, 103–115.
- Reston, T.J., Phipps Morgan, J., 2004. Continental geotherm and the evolution of rifted margins. *Geology* 32, 133–136.
- Reyners, M., Eberhart-Phillips, D., Stuart, G., Nishimura, Y., 2006. Imaging subduction from the trench to 300 km depth beneath the central North Island, New Zealand with  $v_p$  and  $v_p/v_s$ . *Geophysical Journal International* 165, 565–583.
- Rosenbaum, G., Lister, G.S., 2004. Neogene and Quaternary rollback evolution of the Tyrrhenian Sea, the Apennines, and the Sicilian Maghrebides. *Tectonics* 23, TC1013. doi:10.1029/2003TC001518.
- Schellart, W.P., 2004a. Kinematics of subduction and subduction-induced flow in the upper mantle. *Journal of Geophysical Research* 109, B07401. doi:10.1029/2004JB002970.
- Schellart, W.P., 2004b. Quantifying the net slab pull force as a driving mechanism for plate tectonics. *Geophysical Research Letters* 31, L07611. doi:10.1029/2004GL019528.
- Schellart, W.P., 2004c. Three-dimensional fluid dynamic modeling of subduction and mantle flow, Western Pacific Geophysical Meeting Supplement. Eos, *Transactions of the American Geophysical Union* 85 (28), 153 (Honolulu, Abstract T42A-02).
- Schellart, W.P., 2005. Influence of the subducting plate velocity on the geometry of the slab and migration of the subduction hinge. *Earth and Planetary Science Letters* 231, 197–219.
- Schellart, W.P., 2007a. Global trench–migration velocities in different “absolute” reference frames: geodynamic constraints to find the optimal reference frame. EGU General Assembly, Vienna. Abstract EGU2007-A-00648.
- Schellart, W.P., 2007b. The potential influence of subduction zone polarity on overriding plate deformation, trench migration and slab dip angle. *Tectonophysics* 445, 363–372.
- Schellart, W.P., 2008. Kinematics and flow patterns in deep mantle and upper mantle subduction models: Influence of the mantle depth and slab to mantle viscosity ratio. *Geochemistry Geophysics Geosystems* 9, Q03014. doi:10.1029/2007GC001656.
- Schellart, W.P., Lister, G.S., 2004. Tectonic models for the formation of arc-shaped convergent zones and backarc basins. In: Sussman, A.J., Weil, A.B. (Eds.), *Orogenic Curvature: Integrating Paleomagnetic and Structural Analyses*. Geological Society of America-Special Paper, pp. 237–258.
- Schellart, W.P., Freeman, J., Stegman, D.R., 2006. Defining an absolute reference frame for plate motions on Earth from minimizing subduction zone trench migration. *Australian Earth Science Convention*, Melbourne, Extended Abstract, pp. 3.
- Schellart, W.P., Freeman, J., Stegman, D.R., Moresi, L., May, D., 2007. Evolution and diversity of subduction zones controlled by slab width. *Nature* 446, 308–311.
- Schöffel, H.-J., Das, S., 1999. Fine details of the Wadati–Benioff zone under Indonesia and its geodynamic implications. *Journal of Geophysical Research* 104, 13101–13114.
- Sdrolias, M., Müller, R.D., 2006. Controls on back-arc basin formation. *Geochemistry, Geophysics, Geosystems* 7, Q04016. doi:10.1029/2005GC001090.
- Seno, T., Stein, S., Gripp, A.E., 1993. A model for the motion of the Philippine Sea plate consistent with NUVEL-1 and geological data. *Journal of Geophysical Research* 98, 17941–17948.
- Serpelloni, M., Anzidei, M., Baldi, P., Casula, G., Galvani, A., 2005. Crustal velocity and strain-rate fields in Italy and surrounding regions: new results from the analysis of permanent and non-permanent GPS networks. *Geophysical Journal International* 161, 861–880.
- Smalley Jr., R., et al., 2007. Scotia arc kinematics from GPS geodesy. *Geophysical Research Letters* 34, L21308. doi:10.1029/2007GL031699.
- Solomon, S.C., Sleep, N.H., 1974. Some simple physical models for absolute plate motions. *Journal of Geophysical Research* 79, 2557–2567.
- Stegman, D.R., Freeman, J., Schellart, W.P., Moresi, L., May, D., 2006. Influence of trench width on subduction hinge retreat rates in 3-D models of slab rollback. *Geochemistry, Geophysics, Geosystems* 7, Q03012. doi:10.1029/2005GC001056.
- Stegman, D.R., Richards, M.A., Baumgardner, J.R., 2002. Effects of depth-dependent viscosity and plate motions on maintaining a relatively uniform mid-ocean ridge basalt reservoir in whole mantle flow. *Journal of Geophysical Research* 107, 2116. doi:10.1029/2001JB000192.
- Steinberger, B., O'Connell, R.J., 1998. Advection of plumes in mantle flow; implications for hot spot motion, mantle viscosity and plume distribution. *Geophysical Journal International* 132, 412–434.
- Suter, M., Martínez, M.L., Legorreta, O.Q., Martínez, M.C., 2001. Quaternary intra-arc extension in the central Trans-Mexican volcanic belt. *Geological Society of America Bulletin* 113, 693–703.
- Tarduno, J.A., et al., 2003. The Emperor Seamounts: Southward motion of the Hawaiian hotspot plume in Earth's mantle. *Science* 301, 1064–1069.
- Taylor, F.W. et al., in review. Kinematics of the South Shetland Islands–Bransfield basin system, northern Antarctic Peninsula. *Geophysical Research Letters*.
- Taylor, F.W., et al., 1995. Geodetic measurements of convergence at the New Hebrides island arc indicate arc fragmentation caused by an impinging aseismic ridge. *Geology* 23, 1011–1014.
- Thomas, C., Livermore, R., Pollitz, F., 2003. Motion of the Scotia Sea plates. *Geophysical Journal International* 155, 789–804.
- Tregoning, P., et al., 1998. Estimation of current plate motions in Papua New Guinea from global positioning system observations. *Journal of Geophysical Research* 103, 12181–12203.
- Tregoning, P., et al., 1999. Motion of the South Bismarck plate, Papua New Guinea. *Geophysical Research Letters* 26, 3517–3520.
- van der Hilst, R., 1995. Complex morphology of subducted lithosphere in the mantle beneath the Tonga trench. *Nature* 374, 154–157.
- van der Hilst, R., Mann, P., 1994. Tectonic implications of tomographic images of subducted lithosphere beneath northwestern South America. *Geology* 22, 451–454.
- van der Hilst, R.D., Spakman, W., 1989. Importance of the reference model in linearized tomography and images of subduction below the Caribbean plate. *Geophysical Research Letters* 16, 1093–1096.
- van der Hilst, R.D., Engdahl, R., Spakman, W., Nolet, G., 1991. Tomographic imaging of subducted lithosphere below Northwest Pacific island arcs. *Nature* 353, 37–43.
- Van der Voo, R., Spakman, W., Bijwaard, H., 1999. Tethyan subducted slabs under India. *Earth and Planetary Science Letters* 171, 7–20.
- VanDecar, J.C., Russo, R.M., James, D.E., Ambeh, W.B., Franke, M., 2003. Aseismic continuation of the Lesser Antilles slab beneath continental South America. *Journal of Geophysical Research* 108, 2043. doi:10.1029/2001JB000884.
- Vanneste, L.E., Larter, R.D., 2002. Sediment subduction, subduction erosion, and strain regime in the northern South Sandwich forearc. *Journal of Geophysical Research* 107, 2149. doi:10.1029/2001JB000396.
- Vannucchi, P., Scholl, D.W., Meschede, M., McDougall, K., 2001. Tectonic erosion and consequent collapse of the Pacific margin of Costa Rica: combined implications from ODP Leg 170, seismic offshore data, and regional geology of the Nicoya Peninsula. *Tectonics* 20, 649–668.
- Vannucchi, P., Galeotti, S., Clift, P.D., Ranero, C.R., von Huene, R., 2004. Long-term subduction–erosion along the Guatemalan margin of the Middle America Trench. *Geology* 32, 617–620.
- Vergara Muñoz, A., 1988. Tectonic patterns of the Panama Block deduced from seismicity, gravitational data and earthquake mechanisms; implications to the seismic hazard. *Tectonophysics* 154, 253–267.
- Vogt, P.R., 1973. Subduction and aseismic ridges. *Nature* 241, 189–191.
- von Huene, R., Lallemand, S.E., 1990. Tectonic erosion along the Japan and Peru convergent margins. *Geological Society of America Bulletin* 102, 704–720.
- Wallace, L.M., Beavan, J., McCaffrey, R., Darby, D., 2004. Subduction zone coupling and tectonic block rotations in the North Island, New

- Zealand. *Journal of Geophysical Research* 109, B12406. doi:10.1029/2004JB003241.
- Walpersdorf, A., Rangin, C., Vigny, C., 1998. GPS compared to long-term geologic motion of the north arm of Sulawesi. *Earth and Planetary Science Letters* 159, 47–55.
- Wells, R., Weaver, C.S., Blakely, R.J., 1998. Fore-arc migration in Cascadia and its neotectonic significance. *Geology* 26, 759–762.
- Wessel, P., Harada, Y., Kroenke, L.W., 2006. Toward a self-consistent, high-resolution absolute plate motion model for the Pacific. *Geochemistry, Geophysics, Geosystems* 7, Q03L12. doi:10.1029/2005GC001000.
- Widiyantoro, S., Kennett, B.L.N., van der Hilst, R.D., 1999. Seismic tomography with P and S data reveals lateral variations in the rigidity of deep slabs. *Earth and Planetary Science Letters* 173, 91–100.
- Wortel, M.J.R., Spakman, W., 2000. Subduction and slab detachment in the Mediterranean–Carpathian region. *Science* 290, 1910–1917.
- Wright, I.C., 1993. Pre-spread rifting and heterogeneous volcanism in the southern Havre Trough back-arc basin. *Marine Geology* 113, 179–200.
- Yamaoka, K., Fukao, Y., Kumazawa, M., 1986. Spherical shell tectonics: effects of sphericity and inextensibility on the geometry of the descending lithosphere. *Reviews of Geophysics* 24, 27–53.
- Zellmer, K.E., Taylor, B., 2001. A three-plate kinematic model for Lau Basin opening. *Geochemistry, Geophysics, Geosystems* 2 (2000GC000106).
- Zhong, S., Gurnis, M., 1995. Mantle convection with plates and mobile, faulted plate margins. *Science* 267, 838–843.